Distribution and characteristics of supraglacial channels on mountain glaciers in Valais, Switzerland

Holly Wytiahlowsky[1], Chris R. Stokes[1], Rebecca A. Hodge[1], Caroline C. Clason[1], Stewart S.R. Jamieson[1]

[1]Department of Geography, Durham University, Durham, DH1 3LE, United Kingdom

Correspondence to: Holly Wytiahlowsky (holly.e.wytiahlowsky@durham.ac.uk)

Abstract. Supraglacial channels form a key component of glacier hydrology, transporting surface meltwater to englacial and proglacial positions, which impacts ice flow dynamics, surface mass balance and the hydrochemistry of glacial runoff. The presence of supraglacial channels is well-documented on ice sheets using satellite imagery, but much less is known about their properties on mountain glaciers. Here we use high-resolution (0.1 m) orthophotos to identify channels across 285 glaciers in Valais Canton, Switzerland. For the 85 glaciers with visible supraglacial drainage networks, we map 1890 channels (> 0.5 m wide) and investigate their distribution and characteristics. We find glacier hypsometry, size, and slope are good predictors of drainage density, with glaciers characterised by shallow slopes (which have fewer crevasses) and larger snow-free areas (with a high meltwater supply) exhibiting higher drainage densities. The strongest control on drainage density is mean glacier elevation, with glaciers at lower elevations producing higher drainage densities. On average, 80 % of channels drain across the glacier and directly onto proglacial areas, with 20 % terminating englacially. However, there is large inter-glacier variability, with 40 % of glaciers containing no englacially-terminating channels and 3.5 % where all channels terminate englacially. Most channels on glaciers in Valais are slightly sinuous, with higher sinuosities typically occurring in flatter areas and associated with patchy debris cover. Future research should assess the importance of channels below our mapping resolution and network evolution under climate change.

1 Introduction

Glaciers and ice caps are losing mass rapidly (Wouters et al., 2019; Hugonnet et al., 2021; Tepes et al., 2021; The GlaMBIE Team, 2025), resulting in sea level rise, which is anticipated to continue throughout the 21st century and beyond (Bamber et al., 2019; Edwards et al., 2021; Rounce et al., 2023). Glaciers in the lower latitudes (e.g., the European Alps, Caucasus, New Zealand, the USA) are particularly vulnerable to atmospheric warming and may experience complete deglaciation by 2100 under a strong warming scenario (e.g., RCP8.5) (Zekollari et al., 2019; Rounce et al., 2023). In populated mountain regions, these changes will have profound impacts, as glaciers and snowpacks act as vital water towers, supplying freshwater to the 1.9 billion people worldwide who live in or downstream of glacial catchments (Carey et al., 2017; Zemp et al., 2019; Immerzeel et al., 2020; Sommer et al., 2020; Hugonnet et al., 2021; Clason et al., 2023). Glacier meltwater that feeds proglacial rivers is commonly transported to the proglacial margin by supraglacial channels, which are an important component of the glacial

hydrological system. The presence and distribution of supraglacial channels have implications for a range of glacio-hydrological processes as they affect how efficiently meltwater is routed over, through and under glaciers, and can also affect suspended sediment concentrations and hydrochemistry of proglacial rivers. Higher suspended sediment concentrations pose harm to downstream ecosystems and proglacial reservoirs, with concentrations generally higher if meltwater is routed via the bed (Swift et al., 2002), rather than transported across the glacier surface. The presence or absence of channels that route meltwater to the bed also affects the supply of subglacial meltwater, which has implications for subglacial water pressure, the onset of subglacial channelisation and, potentially, ice motion (e.g., Willis, 1995; Jobard and Dzikowski, 2006; Banwell et al., 2016). Despite the importance of meltwater routing, the controls and patterns of meltwater transport on mountain glaciers remain relatively understudied compared to, for example, the Greenland Ice Sheet (GrIS). Notably, it is not yet fully understood why the channelised flow of meltwater occurs on some glaciers but not others (Pitcher and Smith, 2019).

The term 'supraglacial stream' was first coined in the 1970s and 1980s from observations of channels in Scandinavia and the European Alps (e.g., Knighton, 1972, 1981, 1985; Ferguson, 1973; Hambrey, 1977; Seaberg, 1988), with their morphology (i.e., channel shape and structure) often compared to terrestrial streams. However, these early studies only provided small-scale, local observations of channels on individual glaciers. By comparison, a recent revival in supraglacial channel research has primarily focused on large-scale remote-sensing observations of the GrIS (e.g., Smith et al., 2015; Karlstrom and Yang, 2016; Gleason et al., 2021; Yang et al., 2015, 2016, 2018, 2019, 2020, 2021, 2022), and to a lesser extent, Antarctica (e.g., Bell et al., 2017; Kingslake et al., 2017; Chen et al., 2024). Recent remote sensing techniques for channel detection on the GrIS (e.g., Yang and Smith, 2013; King et al., 2016) have rarely been applied to mountain environments, as most channels on mountain glaciers are likely much smaller and therefore fall below the resolution of even the highest-resolution freely available satellite platforms (e.g., Sentinel-2, ~10 m). As a result, it is not known whether the characteristics of channels on ice sheets and the controls on their distribution are comparable to channels on mountain glaciers. The latter are characterised by less available space for channel formation, tend to have a larger debris coverage, and typically contain steeper and more complex topography compared to ice sheet surfaces.

Whilst much remains unknown about supraglacial channel distribution in mountainous environments, previous research has established some fundamental principles (e.g., Knighton, 1972, 1981; Ferguson, 1973; Yang et al., 2016). The formation of supraglacial channels is thought to occur when channel incision via thermal erosion exceeds the rate of surface lowering (Marston, 1983). Channel formation is also influenced by the rate of meltwater production and surface topography, with channels tending to form parallel to the steepest ice flow direction (Irvine-Fynn et al., 2011; Mantelli et al., 2015). Surface topography may reinforce itself, as once an incised channel forms, the higher incision rates may result in an increasingly topographically constrained channel that reactivates annually. At a smaller scale, micro- to macro-scale surface structures have been suggested to influence meltwater routing (Irvine-Fynn et al., 2011), while high supraglacial channel density appears to be correlated with, and may contribute to, increased surface roughness (Rippin et al., 2015). Where channels occur, they are often reactivated annually depending on their depth, with the most deeply incised channels suggested to be a product of high discharge or high slope (St Germain and Moorman, 2019). However, incised channel profiles are not typically uniform, and most channels commonly exhibit asymmetric cross-profiles due to the dominant

direction of solar radiation (St Germain and Moorman, 2019). Additionally, discharge is a strong control on channel form, especially sinuosity, with channels observed to increase in sinuosity throughout the melt season (e.g., Dozier, 1976; Hambrey, 1977; St Germain and Moorman, 2019). Similar to terrestrial river networks, supraglacial channels generally follow Horton's laws, meaning that higher-order channels (i.e., where the highest-order is the main channel) are longer, have lower slopes, and are comprised of a lower number of channel segments (Horton, 1945; Yang et al., 2016). However, much of what we know about supraglacial channels was established from cold to polythermal glaciers or from observations of a small number of individual glaciers (e.g., Knighton, 1972, 1981, 1985; Gleason et al., 2016; St Germain and Moorman, 2019).

In this paper, we investigate a range of potential controls on channel distribution and properties for a large sample of glaciers (n = 285) in a region characterised by high melt rates. We use high-resolution (~0.1 m) orthophoto imagery from 2020 to produce the first comprehensive inventory of 1,890 supraglacial channels in a mountain glacier environment, with a focus on Valais Canton, Switzerland. Our aim is to characterise the morphometry (i.e., quantitative measurements of channel geometry) of supraglacial channels on mountain glaciers, providing insight into where and why they form. This is important for understanding how mass is transported through and away from glaciers, and for determining the extent to which surface hydrological characteristics (e.g., channel transport pathways) are uniform between glaciers, which is beneficial for informing modelling of glacier hydrology and ice motion. Using GIS software, we extract channel metrics (length, sinuosity, slope, elevation, terminus type, proximity to debris) and glacier characteristics (aspect, size, drainage density, elevation, crevassed extent), which are supplemented by qualitative observations. We then explore the relationship between glacier and channel characteristics using statistical measures and infer whether glacier surface characteristics can explain the presence or absence of channels.

2 Study location

Compared to many glacierised regions, Switzerland has the largest repository of high spatial and temporal resolution national LiDAR and orthophoto surveys, providing excellent coverage for the mapping of supraglacial channels. We focus on Valais Canton in southern Switzerland, which contains 303 glaciers over 0.1 km^2, covering a total area of 545 km^2 in 2015 (Fig. 1; Linsbauer et al., 2021). It is the most glacierised Swiss Canton, and in 2015, glaciers in Valais had a mean area of 1.8 km^2, a median of 0.43 km^2 and a maximum area of 77.3 km^2 (Grosser Aletschgletscher) (Linsbauer et al., 2021). We identified Valais Canton as a suitable study site as its glacier size distribution is comparable with Switzerland's as a whole, and the glaciers range from shallow to steep gradients, have differing hypsometries (ice area-elevation distributions), and varying crevasse densities. Thus, this study site captures a wide range of potential influences on channel distributions and characteristics. Valais is comprised of the Bernese Alps to the north and the Pennine Alps in the south, separated by the Rhône Valley (Fig. 1). Glaciers in the Bernese Alps are the largest in the canton and most exhibit a south-to-southeast aspect (mean: 163°). In contrast, the largest glaciers in the Pennine Alps have a north and west aspect (mean: 347°). Glaciers in Valais have an average maximum elevation of 3450 m.a.s.l (min: 2356, max: 4599) and an overall mean elevation of 3091 m.a.s.l (min: 2267, max: 4025).

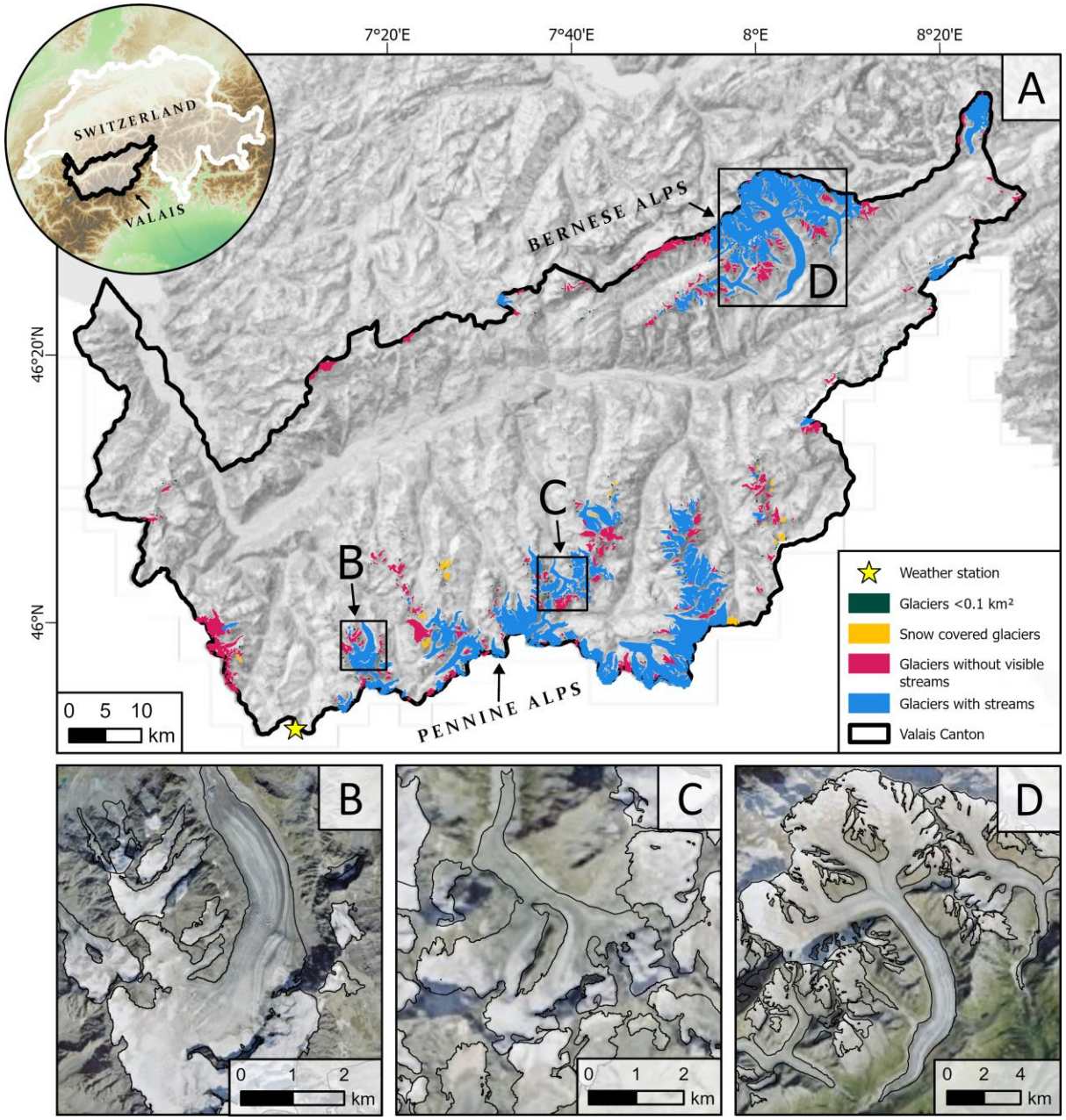

111

112 **Figure 1: The study site area, which contains 303 glaciers > 0.1 km^2. (A) The location of Valais Canton**
113 **(black) is shown within southwest Switzerland. Glaciers containing visible streams (> 0.5 m wide) are shown**
114 **in blue, glaciers without visible streams are in pink, glaciers fully covered by snow are in yellow, and all**
115 **glaciers < 0.1 km^2 (which we omit from this study) are shown in dark green; (B) an example of a large valley**
116 **glacier (Glacier de Corbassière), with smaller glaciers at higher elevations; (C) the debris-covered tongue**
117 **of Glacier du Grand Cornier and surrounding smaller glaciers; and (D) the larger glaciers (e.g., Grosser**
118 **Aletschgletscher, centre right) in the north of Valais. The location of Col du Grand St-Bernard**
119 **meteorological weather station is indicated by a yellow star. Glacier outlines used are from the Swiss Glacier**
120 **Inventory (SGI2016), with glacier extent shown for 2015-16. The outlines are overlayed on basemap**
121 **imagery sourced from Esri (2024).**

122

Within Valais, the only meteorological station with a similar elevation to many glacier termini is Col du Grand St-Bernard (2472 m.a.s.l) in the Pennine Alps (Fig. 1), which (between 1991 and 2020) recorded mean July air temperatures (2 m) of 8.4 °C, mean January temperatures of -6.9 °C, and mean annual temperatures of -0.1 °C. At Col du Grand St-Bernard, July averages 140 mm of precipitation (1991-2020), with 12.7 days a month experiencing > 1 mm of precipitation, compared to a January average of 242 mm across an average of 12.9 days. However, Switzerland's climate is changing and mean air temperatures between 2013 and 2022 were 2.5 °C warmer than pre-industrial temperatures (MeteoSwiss, 2024), which has greatly impacted the mass balance of Swiss glaciers in recent decades (Fischer et al., 2015; Davaze et al., 2020).

3 Methods

3.1 Imagery acquisition and channel delineation

The method commonly used for automated channel detection, developed by Yang and Smith (2013) for delineating water bodies on the GrIS from WorldView-2 imagery (1.84 m), uses a normalised difference water index adapted for ice ($NDWI_{ice}$). Following Yang and Smith (2013), we applied a modified $NDWI_{ice}$ approach to a high-resolution (0.1 m) orthophoto tile (1 km by 1 km) on the Grosser Aletschgletscher. However, our $NDWI_{ice}$ output predominantly detected water-filled crevasses, and whilst it was able to detect some channels > 0.5 m in width, it typically identified only the largest channels (mostly > 1 m). It also missed many channels that were visible but contained very small amounts of water, or incised channels where the water surface was not visible. This method is likely better suited to coarser imagery (less visible crevasses) in less complex terrain and/or for simply using a threshold to extract higher-order channels. As a result, we undertook manual mapping, which in some instances is sevenfold more accurate in ascertaining channel density compared to automated methods (King et al., 2016).

We obtained high-resolution cloud-free orthophoto imagery (0.10 m resolution) from SwissTopo (swisstopo.admin.ch), with acquisition dates during mid-July 2020. Imagery was not available for later in the melt season, which lasted from approximately April to September 2020 at Col du Grant St Bernard. Hence, our data is unlikely to capture the peak extent of channel distribution, which is expected to occur in late summer. Snow conditions at Col du Grand St-Bernard in mid-July were likely to be lower than average, as the precipitation of the preceding winter (total across December, January, February) was 570 mm compared to the 2010 to 2020 mean of 704 mm. May temperatures were slightly warmer than average (2020 mean: 3.4˚C; 2010-20 mean: 1.7˚C), followed by a colder than average June (2020 mean: 4.8 ˚C; 2010-2020 mean: 6.3 ˚C), meaning that whilst there was less snow, it may have melted more slowly than previous years.

We first removed all glaciers in Valais smaller than 0.1 km^2 from our study sample (582 reduced to 303 glaciers). This is because they are likely too small to produce large enough channels to be detected by our imagery, and because many small glaciers in the Swiss Glacier Inventory (SGI2016) are unlikely to meet the criteria to be identifiable as glaciers (Leigh et al., 2019). Due to the date of imagery acquisition, 6 % of the remaining 303 glaciers were still completely snow-covered and were omitted from further analyses as the presence or absence of channels could not be detected, leaving 285 glaciers. Within these glaciers, the mean snow-free area was 38.9 % in mid-July 2020, with some variation in snow cover at different elevation bands. For example, glaciers with a

mean elevation between 2500 - 2800 m.a.s.l had a 45.0 % snow-free area on average, compared to 36.6 % at 3100 - 3400 m.a.s.l. The lowest percentage of snow-free area was 4.9 % at a high elevation cirque, and five glaciers were completely snow-free by mid-July but were all under 0.7 km^2.

Each glacier was systematically surveyed for supraglacial channels in *QGIS* (e.g., Fig. 2). Of the 285 glaciers that we surveyed, 85 supported supraglacial channels above our mapping threshold. Only channels confidently visible at a 1:1,000 scale were delineated for the purpose of consistency, meaning the minimum channel width we delineated was ~0.5 m. We solely focus on these larger channels because of difficulties in delineating small channels objectively, which include problems with differentiating complex rill networks from structural features (e.g., fractures). Additionally, smaller channels may have widths that periodically fall below the pixel resolution, which may require subjective judgments to be made. Whilst we do not map channels below the scale defined above, many of the glaciers likely contain smaller channels that are not sufficiently clear enough to map. These smaller channels may form a key hydrological component of these glaciers, but we anticipate that the channels we have mapped carry the bulk of the meltwater. Individual channels were mapped from their downstream end until they were no longer clearly visible or when channels could not be confidently and objectively mapped. When channels have tributaries above the mapping resolution, the main channels are mapped as one segment, continuing up the largest channel at each confluence. Each tributary channel was then subsequently mapped as a new individual segment. Once mapped, each entire channel segment was assigned a code based on its attributes and whether it was on bare ice, surrounded by patchy debris, or on a debris-covered part of the glacier. The type of terminus was assigned to each channel, which was one of: running off the glacier terminus, terminating in a moulin, crevasse, lake, the glacier periphery, adjoins another channel, or disappears beyond the resolution (i.e., the terminus is not visible and cannot be confidently inferred).

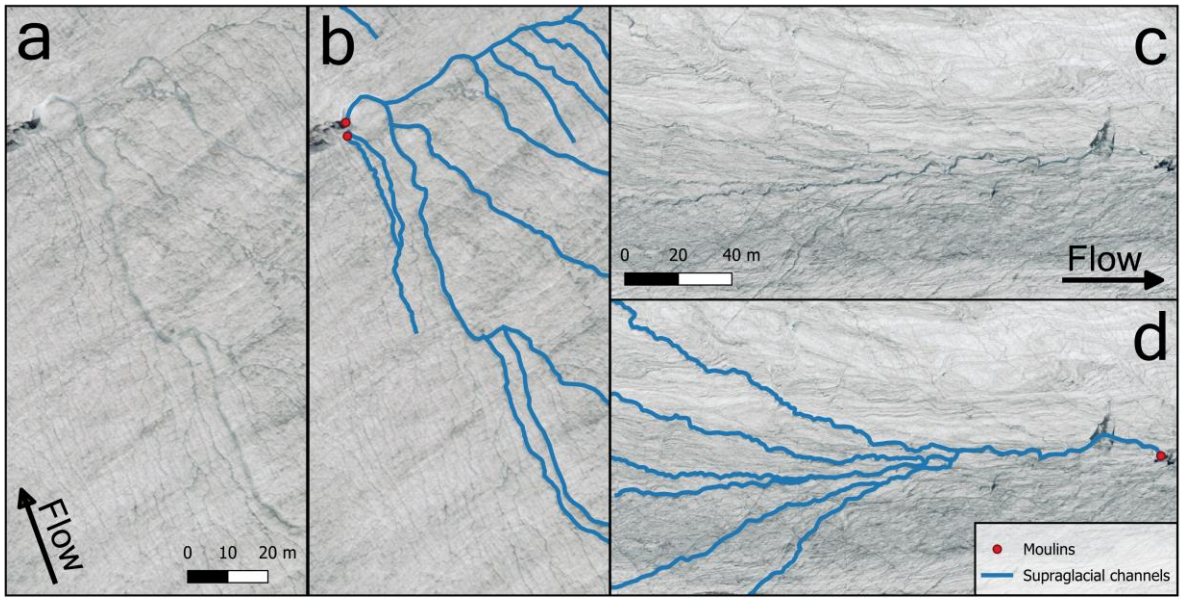

Figure 2: Examples of the mapped output and corresponding orthophoto. Channels are shown in blue, and moulins are represented by red circles when a mapped channel is moulin-terminating. Arrows indicate the direction of ice flow. (a-b) Supraglacial channels on the Glacier de Moiry and (c-d) Allalingletscher. Imagery source: Federal Office of Topography Swisstopo.

To ensure consistency, all mapping and the error assessment were conducted by the same individual. We quantified the repeatability of our mapping by delineating channels from the same image of the Rhonegletscher on two occasions, months apart. This revealed a 2.6 % difference in calculated drainage density and a 0.21 % decrease in total channel length from the original mapping (Figure B1). The error from our repeat mapping may have been lower if the mapping had been repeated immediately after the original mapping, whereas the original mapping was conducted consistently over a time period. However, the error margin is small enough for us to conclude that the original mapping provided a good representation of each glacier's drainage density. Both sets of mapping also clearly identified where channels terminate. The primary source of uncertainty here stems from knowing when to stop mapping up-channel and total channel length. We therefore took a conservative approach to avoid over-interpreting channel pathways and only mapped the up-glacier limit of channels where we are confident that it exists.

3.2 Metrics

A total of 1890 channel segments (polylines) were mapped across the glaciers that contained channels. We then used the high-resolution (0.5 m) SwissALTI3D DEM (2019) from swisstopo.admin.ch (1 sigma accuracy of ± 0.3 m for each dimension) to extract morphometric characteristics from each channel segment. The DEM is coarser than the orthophotos used for channel delineation, and there is a one-year offset between their acquisition dates. However, as the DEM is used to calculate larger-scale metrics such as elevation and slope, the small offset is unlikely to affect overall results. Extracted channel metrics were segment length, straight line distance, elevation (minimum, maximum), elevation difference, and channel slope. The start and end points of each segment were then used to derive the sinuosity of each segment (channel length/straight line distance) and drainage density for each glacier (total length of channels/glacier area). We used the glacier snow-free area at the time of mapping to calculate drainage density, which resulted in a higher value than if the entire glacier area had been used.

Glacier characteristics were obtained from the Swiss Glacier Inventory (SGI2016), which included glacier area, aspect, and elevation (minimum, maximum and mean) in 2015 (Linsbauer et al., 2021). This record is the most up-to-date record of Swiss glacier area, but glaciers have since undergone substantial recession. Glacier slope values from the SGI2016 cannot be used as they encompass the whole glacier, whereas for our analysis, we wanted to measure the slope of the snow-free portion of the ablation area at the time of channel mapping. To calculate slope values, each glacier polygon was clipped to its snow-free area, and then zonal statistics in *QGIS* were used to extract the mean, minimum and maximum slope value from the SwissALTI3D DEM for each polygon. The snow-free slope value is the only glacial slope value used in data analyses. We assigned codes to each glacier based on the size of the crevassed area due to its potential impact on channel formation. This included the following classes: little to no (less than 10 % of the snow-free area), moderate (10-50 % covered), and heavily crevassed (covers > 50 % of the snow-free area).

3.3 Statistical tests

To determine whether there is a relationship between channel morphometry and glacier characteristics, we produced a correlation matrix using Spearman's rank correlation (ρ) (e.g., St Germain and Moorman, 2019). Each metric used in this analysis comprises 1890 values, each representing an individual channel segment. The analysis used the following channel variables: segment length, channel slope, sinuosity, minimum elevation, maximum elevation and elevation range, and the following glacier variables: drainage density, glacier area, mean slope of the snow-free area, aspect, glacier minimum elevation, glacier mean elevation, and glacier maximum elevation. For each of the glacier variables, all channel segments on the same glacier were allocated the same value. A singular ANOVA test was conducted to determine the significance of the relationship between debris cover and sinuosity, as an ANOVA test is best suited to determining if there is a significant difference between different classes of debris cover. We also conducted a Principal Component Analysis (PCA) to determine the relationship between variables and to identify drivers of variance amongst the dataset, with data normalised to aid in identifying patterns within the data.

4 Results

4.1 Glacier observations

Glaciers with channels (n = 85) have a larger mean area than glaciers without channels (n = 200) (mean area = 5 km^2 vs. 0.6 km^2) and all glaciers larger than 5.6 km^2 contain channels > 0.5 m wide (Table 1, Fig. 3a). However, the modal glacier area is 0.1 to 1 km^2 for glaciers both with and without visible channels (Fig. 3a). Glaciers containing channels typically have lower slopes compared to those without channels (mean slope: 21° vs. 28°) (Fig. 3b). Glaciers with channels generally have longer tongues that terminate at lower elevations (mean minimum elevation = 2797 m vs. 2936 m) and have higher maximum elevations (mean max elevation = 3637 m vs. 3555 m). The mean drainage density on glaciers with channels is 2.4 km/km^2 and a maximum of 15.2 km/km^2. The latter was found on Oberer Theodulgletscher, which has the lowest glacier slope in the dataset (13°) (Fig. 3c, Fig. 4a).

Table 1: Glacier and channel characteristics.

	Channel Length (m)	Channel Slope (°)	Sinuosity	Drainage Density (km/km^2)	Mean Glacier Slope (°)	Glacier Area (km^2)
Count	1890	1890	1890	85	85	85
Minimum	5.2	0.8	1.0	0	10.4	0.1
Median	152.2	6.3	1.1	1.5	20.6	1.5
Mean	211.7	8.0	1.1	2.4	21.0	5.0
Maximum	4314.4	47.8	3.8	15.3	43.0	83.0
Range	4309.3	47.0	2.8	15.2	32.6	82.9
Standard Deviation	228.3	6.3	0.1	2.6	6.5	10.7
Standard Error	5.3	0.1	0.0	0.3	0.7	1.2
Kurtosis	65.8	7.4	153.0	9.0	1.1	35.3
Skewness	5.5	2.3	9.5	2.6	0.8	5.4

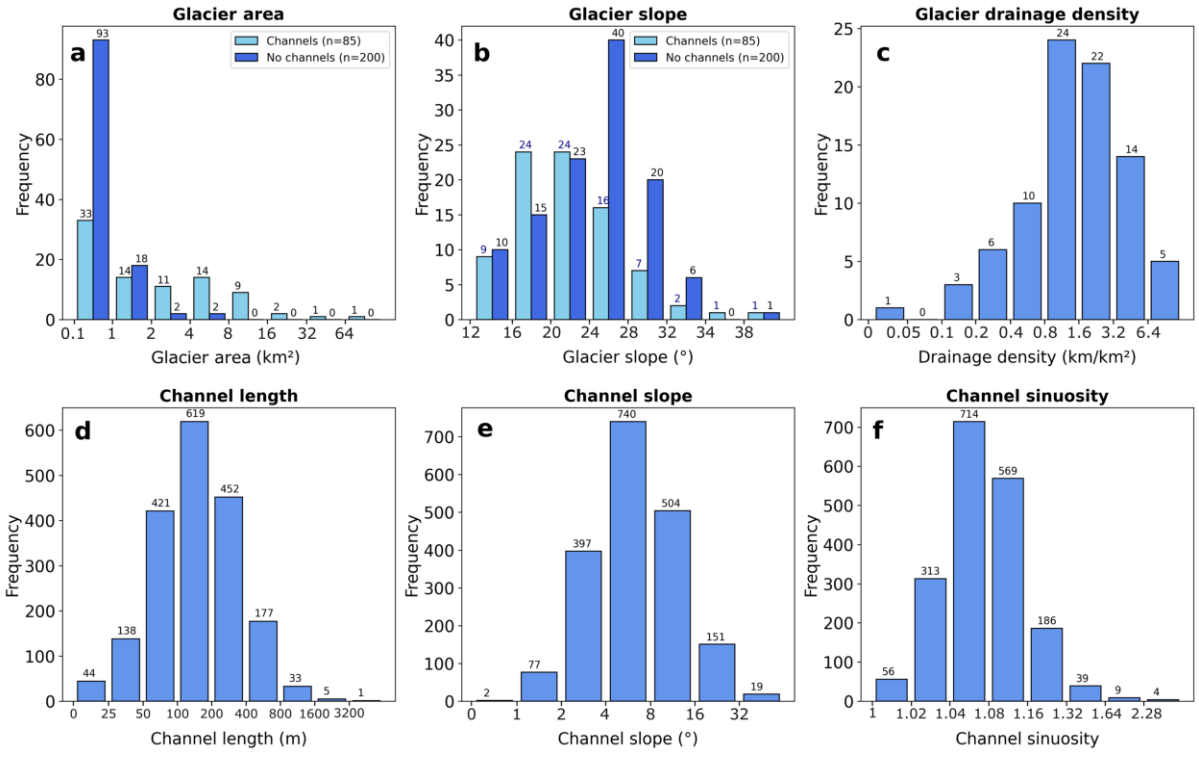

Figure 3: Histograms of extracted metrics. Note that the x-axis uses a log scale (except for Fig. 3b) and the numbers above each bar represent the number of channels/glaciers within each class. The range shown by each bar is indicated by the x-axis values to either side. The range is exclusive of the lower value and inclusive of the higher one (e.g., > 1 - ≤ 2). (a) Glacier area (km^2); (b) glacier slope (°); (c) glacier drainage density (km/km^2); (d) channel segment length (m); (e) channel slope (°); and (f) channel sinuosity.

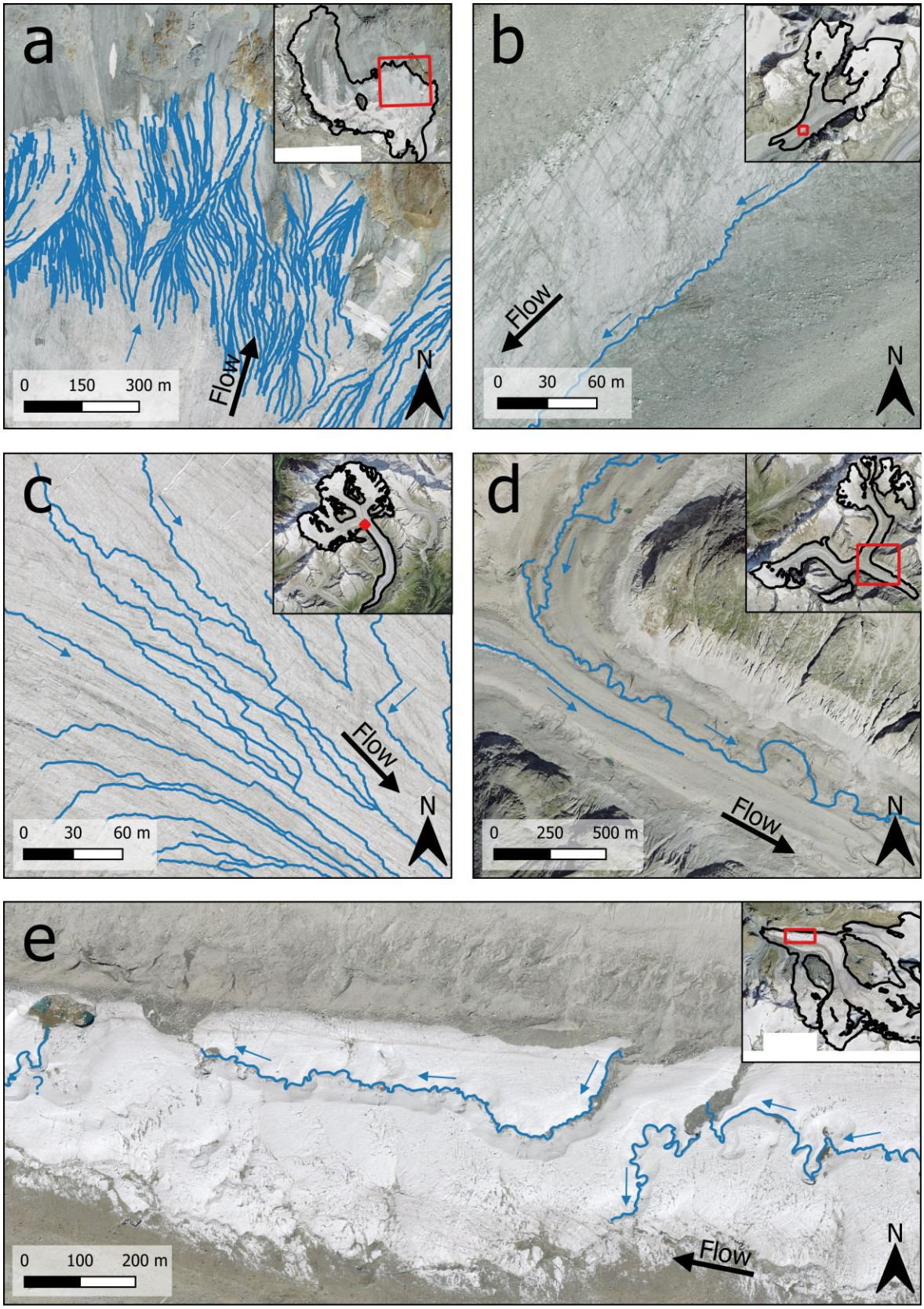

264

265 **Figure 4: Examples of supraglacial channels. Channel location is shown in relation to the whole glacier in**
266 **the top right of each panel, with the panel extent shown in red. (a) Channels on the Oberer**
267 **Theodulgletscher; (b) a channel at the interface between bare ice and debris-covered ice on Glacier du**

Brenay; (c) channels on the Grosser Aletschgletscher - note the straight segments where crevasses have been exploited; (d) channels on the debris-covered terminus of the Oberaletschgletscher; and (e) sinuous channels towards the terminus of Gornergletscher, including an example of a small supraglacial lake (left). The black arrows indicate the glacier flow direction, and the blue arrows indicate the water flow direction. A question mark is shown when the water flow direction is unclear in the DEM. Imagery source: Federal Office of Topography, Swisstopo.

4.2 Channel characteristics

Individual channel segments have a mean length of 212 m, with a positively skewed leptokurtic distribution (Fig. 3d; Table 1). Few segments exceed 1,600 m, as the snow-free areas of most glaciers are smaller than this. The channel segments have a mean slope of 8°, and most exhibit a slope between 4 and 16° (Fig. 3e; Table 1). The maximum channel slope is 48°, but the overall distribution is positively skewed towards smaller slope values. The sinuosity index of each channel ranges from 1 (straight line) to a maximum of 3.8, with a mean value of 1.1, which is classified as sinuous (1.05 - 1.25), but not high enough to be defined as meandering (> 1.25) (Table 1) (Brice and Blodgett, 1978). Sinuosity is the most positively skewed variable, with a highly leptokurtic distribution, as most channels are not very sinuous (Fig. 3f).

Channels terminate in a range of settings, with 47 % joining another channel, 15 % terminating in crevasses, 14 % terminating in moulins, 13 % disappearing below the mapping resolution, 8 % running off at the glacier terminus, 2 % running off the side of the glacier, and 1 % terminating in a supraglacial lake (e.g., Fig. 4e). When only considering terminal segments (i.e., channels not adjoining another channel or disappearing below the mapping resolution), 72 % of segments terminate englacially (crevasses or moulins), 25 % run-off (terminus or periphery), and 3 % terminate in a supraglacial lake. However, larger glaciers with higher drainage densities disproportionately impact these values. For example, 582 out of the 1890 mapped channel segments are on the Grosser Aletschgletscher, where no visible channels reach the terminus; hence, englacially terminating channels may be overrepresented by a single glacier. By comparison, the average glacier within our dataset is characterised by 80 % of channels terminating proglacially and 20 % terminating englacially. Overall, 48 % of glaciers have no englacially-terminating channels, with only 3.5 % of glaciers solely containing englacially terminating channels.

Qualitative observations suggest that channel distribution and morphology are controlled by glacier structure and topography. For example, channels often occur along the interface between debris-covered and bare ice (e.g., Fig. 4b), particularly adjacent to medial moraines, where channels are confined to a topographic depression, commonly occurring at the confluence between two tributaries. The influence of glacier structure on channel morphology is also observed where trace or shallow crevasses are exploited to produce long, straight channel sections (e.g., Fig. 4c). By comparison, the most sinuous channels tend to occur at low elevations on large glaciers characterised by larger flat areas towards to their terminus (Fig. 4e).

4.3 Relationships between channel and glacier characteristics

Here, we investigate links between different supraglacial channel and glacier characteristics. Previous studies informed our choice of variables tested for potential relationships, with a focus on how glacier properties (slope, area and elevation) affect glacier drainage density (e.g., Yang et al., 2016) and channel morphometry, such as sinuosity and channel segment length (e.g., St Germain and Moorman, 2019). We find that the most sinuous channels are more likely to occur on shallow slopes (0 to 10°), with channels on steeper slopes (> 20°) unlikely to exhibit a sinuosity over 1.3 (Fig. 5a). Statistically significant differences in channel sinuosity are also observed between our debris classes ($p < 0.05$; one-way ANOVA) (Fig. 5c). Channels on patchy ('proximal') debris cover tend to be the most sinuous and are statistically different ($p < 0.05$; Tukey Honest Significant Difference test) from channels on continuous debris cover ('debris') and those on bare ice ('clean'). The 'debris' class is generally more sinuous than the 'clean' class, but this difference is not statistically significant. Additionally, channel segment length tends to increase on shallower slopes (Fig. 5b). This relationship is clearly defined by an upper limit, where channels > 500 m are confined to slopes of < 20˚ and no channels occur on slopes > 50˚, except for one outlier (Fig. 5b). Channel segments that terminate in moulins tend to be the longest (mean: 341 m, max: 1999 m), followed by channels that disappear below the mapping resolution (mean: 259 m, max: 4314 m), and then channels reaching the glacier terminus (mean: 214 m, max: 1193 m) (Fig. 5d). The very few (1 %) channels that terminate in supraglacial lakes tend to be short (mean: 109 m, max: 260 m), as do channels that adjoin a higher-order channel (mean: 169 m, max: 1174 m) (Fig. 5d).

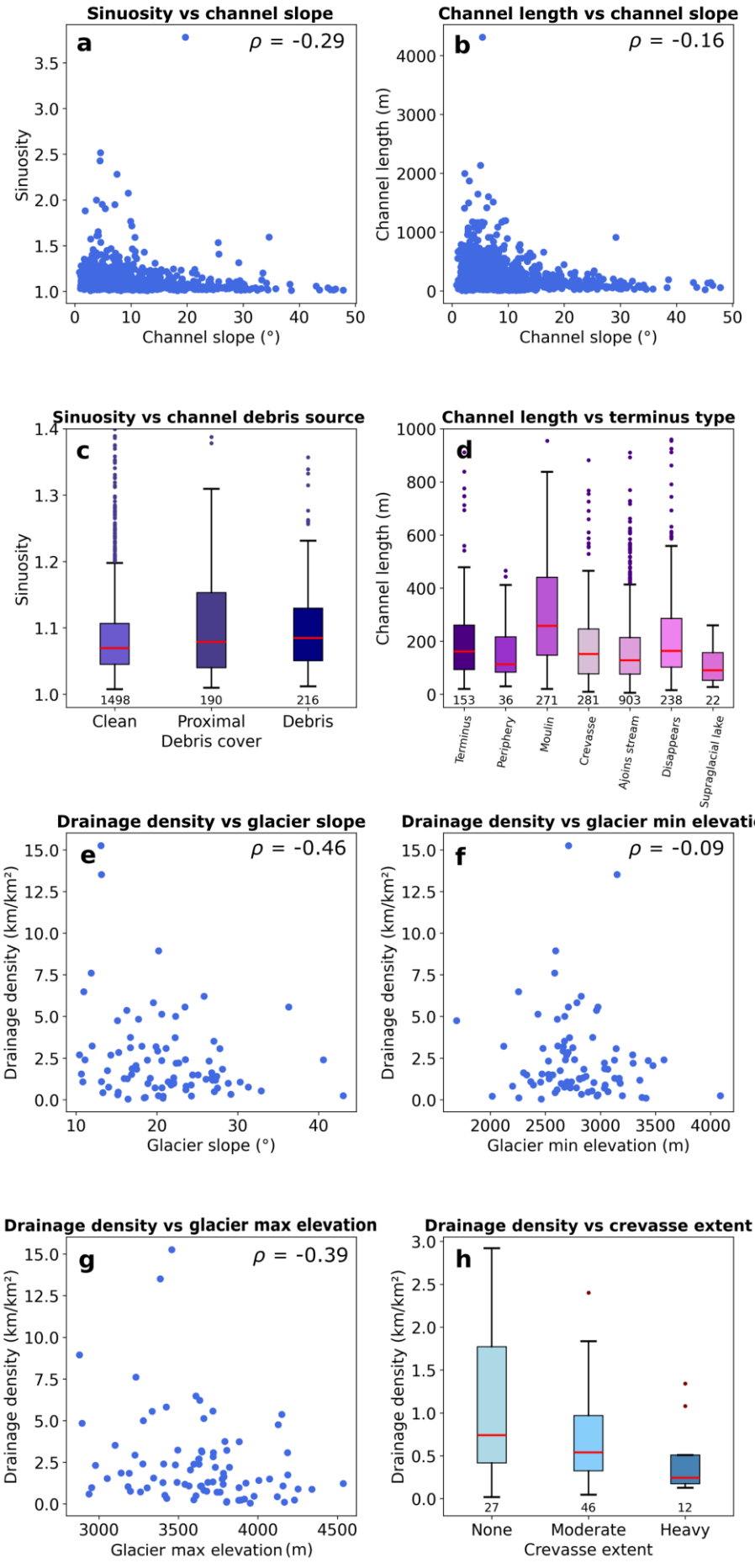
Sinuosity vs channel slope
a
ρ = -0.29
Sinuosity
Channel slope (°)
Channel length vs channel slope
b
ρ = -0.16
Channel length (m)
Channel slope (°)
Sinuosity vs channel debris source
c
Sinuosity
1498
190
216
Clean
Proximal
Debris
Debris cover
Channel length vs terminus type
d
Channel length (m)
153
36
271
281
903
238
22
Terminus
Periphery
Moulin
Crevasse
Ajoins stream
Disappears
Supraglacial lake
Drainage density vs glacier slope
e
ρ = -0.46
Drainage density (km/km²)
Glacier slope (°)
Drainage density vs glacier min elevation
f
ρ = -0.09
Drainage density (km/km²)
Glacier min elevation (m)
Drainage density vs glacier max elevation
g
ρ = -0.39
Drainage density (km/km²)
Glacier max elevation (m)
Drainage density vs crevasse extent
h
Drainage density (km/km²)
27
46
12
None
Moderate
Heavy
Crevasse extent

321

Figure 5: Relationships between channel characteristics (a-d) and glacier metrics (e-h). Plots a-d contain data from 1890 channels, and plots e-h contain data for the 85 glaciers with visible channels. Spearman's rank (ρ) values are included for all scatterplots, each of which is statistically significant ($p < 0.05$). (a) Sinuosity vs channel slope (°); (b) channel segment length (m) vs channel slope (°); (c) sinuosity vs channel debris source; (d) channel segment length (m) vs terminus type; (e) drainage density (km/km^2) vs glacier slope (°); (f) drainage density (km/km^2) vs minimum glacier elevation; (g) drainage density (km/km^2) vs maximum glacier elevation; and (h) drainage density (km/km^2) vs crevasse extent.

Relationships between glacier metrics (Fig. 5e-h) are less clear than for channel characteristics (Fig. 5a-d), which may be due to the lower number of data points (85 glaciers compared to 1890 channels). However, a moderate negative correlation between drainage density and glacier slope exists, with the highest drainage densities occurring on the lowest surface slopes (Fig. 5e). A relationship between drainage density and minimum glacier elevation is less obvious (Fig. 5f), but there appears to be a peak in drainage density between 2600 and 3100 m.a.s.l, which would require further validation from a larger sample of glaciers. By comparison, there is less evidence of a relationship between glacier drainage density and maximum glacier elevation (Fig. 5g). Likewise, there is no statistically significant relationship between glacier aspect and drainage density (Kruskal-Wallis test: $p = 0.61$). Glacier drainage density also tends to be higher on glaciers containing fewer crevasses (Fig. 5h).

4.4 Spearman's rank and Principal Component Analysis

We examined the controls on channel morphometry and drainage density by calculating a correlation matrix. We use Spearman's rank correlation (ρ) and significance values (p), as many of our relationships are not linear. Given our large dataset and the fact that most p-values are < 0.05, even modest correlations are statistically significant and likely reflect genuine relationships.

The strongest control on glacier drainage density is glacier mean elevation ($\rho = -0.66$, $p \leq 0.001$), with higher drainage densities observed when a larger portion of glacier area exists at lower elevations (Fig. 6), followed by glacier mean slope ($\rho = -0.46$, $p \leq 0.001$). This is consistent with Figure 5e, where the highest drainage densities are observed at glaciers with very low slope angles (e.g., Oberer Theodulgletscher; Fig. 4a).

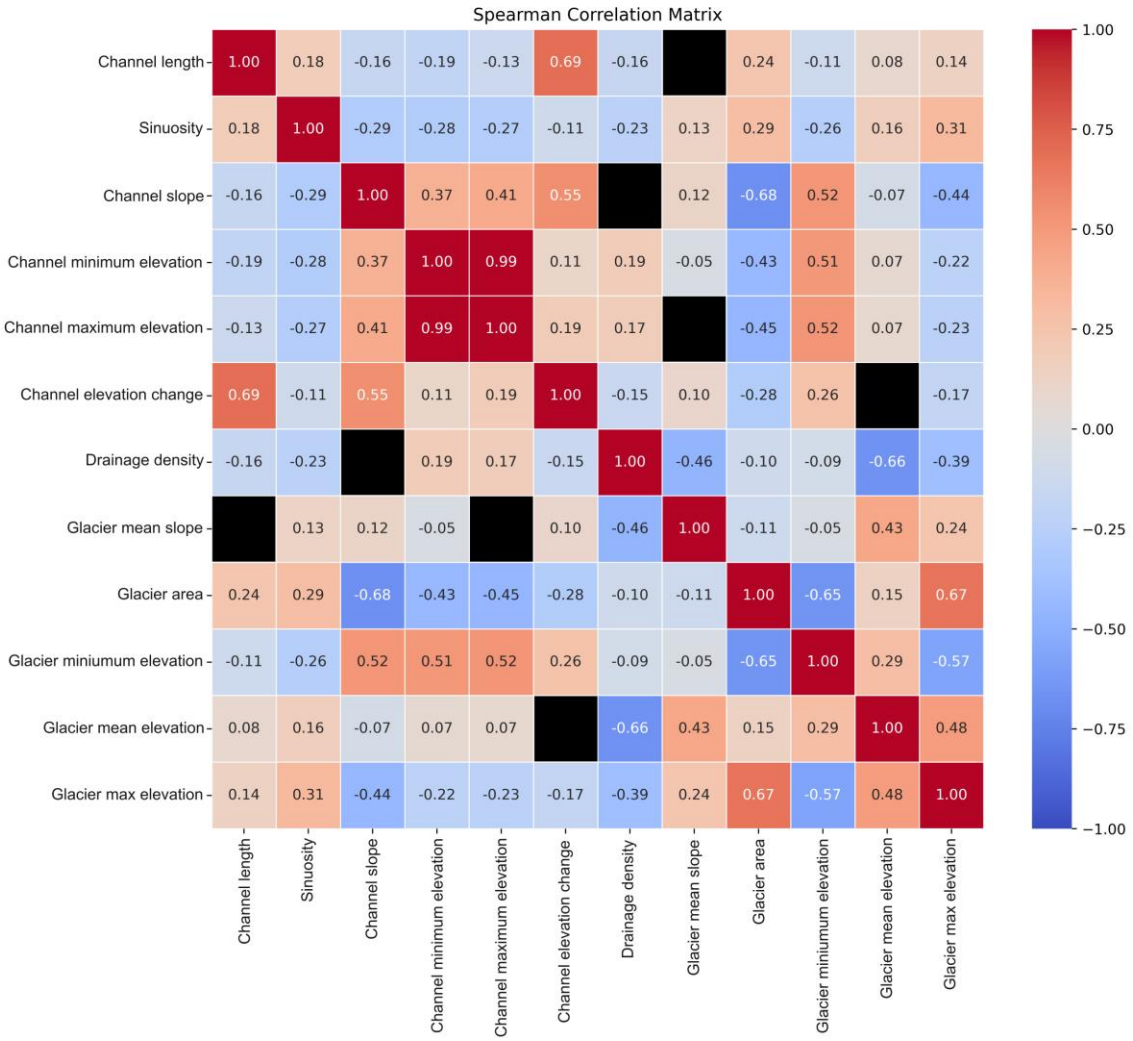

Figure 6: A heatmap matrix of Spearman's rank correlation showing the relationship between glacier and channel characteristics. Correlation values are scaled along a colour ramp, and non-significant relationships (p > 0.05) are coloured black.

By comparison, channel morphometry is characterised by more complex and weaker relationships between variables. For example, high channel sinuosity can in part be explained by multiple weak correlations: sinuosity values tend to increase with a decrease in channel slope (ρ = -0.29, $p \leq 0.001$), and the most sinuous channels occur on larger glaciers (ρ = 0.29, $p \leq 0.001$) with lower minimum elevations (ρ = -0.26, $p \leq 0.001$) (Fig. 6). Channel slope is primarily controlled by glacier characteristics, with higher slope channels mostly existing on smaller glaciers (ρ = -0.68, $p \leq 0.05$), which terminate at higher elevations (ρ = 0.52, $p \leq 0.05$), meaning the steepest channels are likely found at high elevation cirques and hanging glaciers.

To assess the relationship between variables and determine the drivers of variance, we conducted a Principal Component Analysis (PCA). The PCA loadings show that glacier area has a large negative loading on principal component 1, closely followed by strong positive loadings from minimum glacier elevation and channel elevation

(maximum and minimum) (Table A1). By comparison, principal component 2 shows a strong positive loading from drainage density, and large negative loadings from mean glacier slope and glacier mean elevation (Table A1). The first two components explain 50 % of the variance within the dataset, with an additional 13 %, 12 % and 9 % explained by principal components 3, 4, and 5, respectively, which together explain 84 % of the variability (Table A1). Given the complexity of the dataset, our analysis reveals no clear visual clustering of data, but the PCA loadings show an expected relationship between elevation variables and slope variables. However, drainage density is not closely related to any other variable (Fig. A2). Overall, our PCA analysis reveals no single, primary driver of variance; instead, it is apparent that there is a complex, yet interlinked relationship between all variables that explain the distribution and appearance of supraglacial channels.

5 Discussion

5.1 Controls on the spatial distribution of channels

Of the 285 glaciers in our study area, 85 contained channels (> 0.5 m) visible in high-resolution imagery (0.1 m) from mid-July 2020. The presence of visible channels is primarily controlled by a combination of sufficient meltwater supply and distance for meltwater to coalesce and incise. Hence, in Valais, channels are infrequently detected on cirque glaciers due to their smaller snow-free area, steeper and often crevassed slopes, and limited distance for meltwater to coalesce. These cirque glaciers may contain channels below our mapping resolution; however, they cannot be reliably quantified as part of this study. Glaciers containing channels tend to be larger, resulting in the production of more surface melt. We found that all glaciers in Valais larger than 5.6 km^2 supported channels and that glacier area controls much of the variability within the dataset (Table A1), albeit with large variation in drainage density. This variation is in part attributed to glacier slope, which, together with ice flow velocity, governs the crevassed area of a glacier. This crevassed zone, in turn, controls the area in which channels can form. For example, when crevasses are open, they can intercept meltwater, inhibiting the formation of longer channels. Conversely, closed crevasses can add small-scale variability to surface topography, routing meltwater along crevasse traces. Channel formation is also governed by glacier hypsometry, with glaciers containing a larger portion of their area at lower elevations more likely to have higher drainage densities due to a larger snow-free area (Fig. 6). We assume that our images from mid-July do not capture the maximum channel extent on higher elevation glaciers. However, regardless of the image acquisition date, channel density will likely remain highest at lower elevations where surface melt is greater.

The schematic in Figure 7 depicts how glacier elevation and hypsometry are likely to influence the distribution and density of supraglacial channels in alpine settings. The lowest drainage densities are predicted to occur on smaller cirque glaciers due to their lower meltwater supply, restricted distance for meltwater to coalesce into channels, and increased channel interception due to crevasses on often steeper slopes (Fig. 7A). Whilst we detect very few channels on cirques due to our imagery resolution, these glaciers likely still contain networks of smaller channels. By comparison, larger valley glaciers (e.g., Grosser Aletschgletscher) tend to exhibit moderate to high drainage densities because they produce high amounts of meltwater, but much of it may be intercepted by crevasses on steeper slopes, preventing or restricting large channel formation (Fig. 7B). The glaciers with the

highest drainage densities are likely to have a large snow-free area (high meltwater supply) and occur on lower slopes because fewer crevasses allow large drainage networks to become established (Fig. 6; Fig. 7C). One example of this configuration is the Oberer Theodulgletscher which has the highest drainage density among Valais glaciers (Fig. 4a). It is possible that its high drainage density is also due to its location on a high elevation plateau, because air temperatures are likely to be cooler than at the termini of neighbouring glaciers which extend further down valley (Fig. 5f). As a result, the rate of surface lowering is likely slower, meaning that lower rates of incision are needed for channel formation to keep pace with surface lowering, resulting in a higher drainage density (Pitcher and Smith, 2019). However, summer temperatures in the Alps are increasing (Sommer et al., 2020), which will result in higher rates of surface lowering, meaning that all glaciers, but more specifically those with larger portions of their area at lower elevations, will require increased channel incision to counteract the higher rates of surface lowering (Marston, 1983).

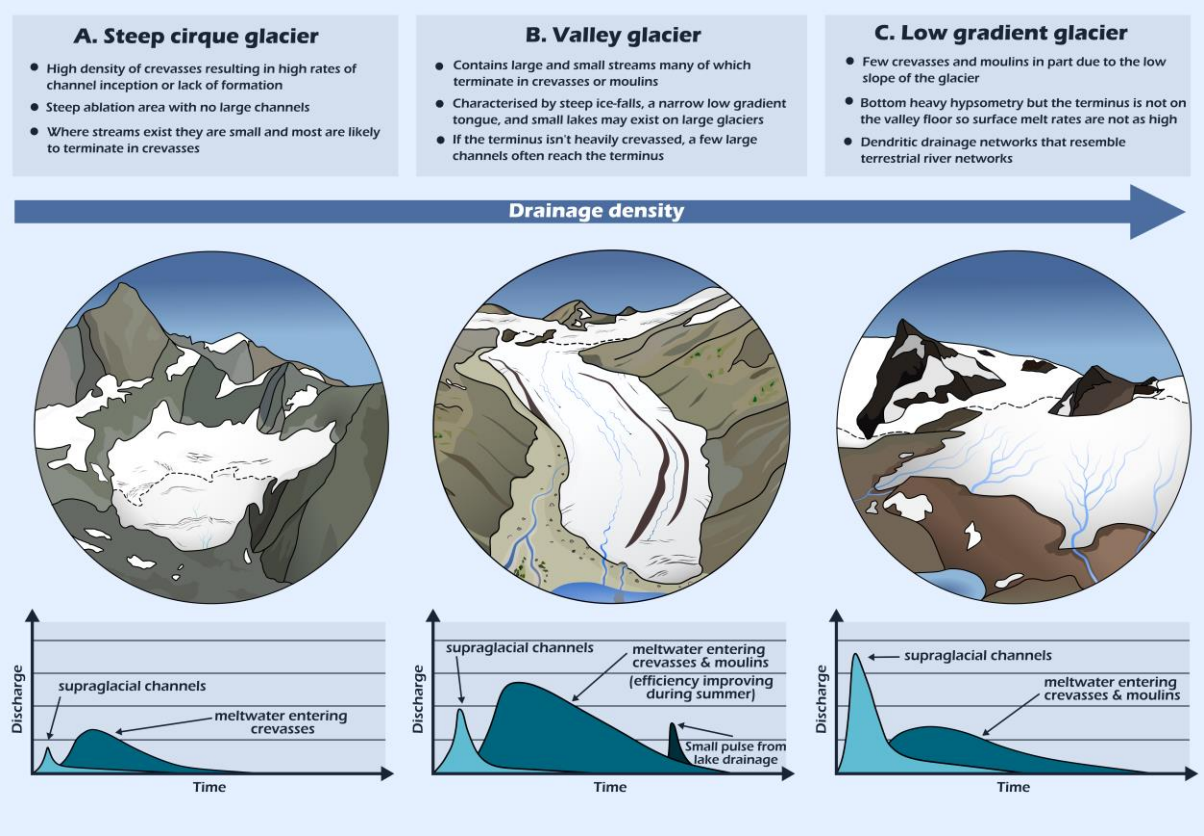

Figure 7: A schematic depicting the range of glacier types (A-C) and their respective characteristics, increasing in drainage density from left to right. Each glacier type corresponds to a hypothesised hydrograph (bottom) depicting changes in proglacial channel discharge over an unknown time period (ranging from minutes to days) as a response to a surface melt event. The hydrographs are hypothesised to represent the general characteristics of each glacier's runoff regime (see text for discussion) and do not reflect the complexities of individual measured proglacial stream discharge. Light blue shading shows the hypothesised hydrograph if all the meltwater were to be transported via supraglacial channels, whereas

those shown in medium blue show the hydrograph where the bulk of meltwater is transported englacially/subglacially. Dark blue in panel (b) shows a lake drainage event.

The distribution and density of channels on different types of glaciers will likely impact the runoff hydrograph (Fig. 7). At small cirque glaciers, runoff in response to surface melt is likely characterised by a small earlier peak from a few supraglacial channels (light blue shading in Fig. 7A) or a slightly delayed peak as crevasses capture meltwater and route it through the en- (and -sub) glacial drainage systems (medium blue shading in Fig. 7A) (e.g., Clason et al., 2015). By comparison, valley glaciers are larger and tend to contain more supraglacial channels, but channels are often intercepted by crevassed zones or ice falls. This may result in an initial peak in meltwater from supraglacial channels, followed by a delay in meltwater routed en- (and sub-) glacially (Fig. 7B). Over the melt season, the lag time between melt and peak proglacial discharge typically decreases due to increased subglacial drainage network efficiency (Nienow et al., 1998). Additionally, some larger valley glaciers contain small supraglacial and ice marginal lakes (e.g., Gornergletscher and Grosser Aletschgletscher), which may experience infrequent drainage events (e.g., Huss et al., 2007), leading to a sudden peak in proglacial river discharge. Whilst less common in Valais, glaciers characterised by large shallow sloping areas often contain extensive supraglacial drainage networks that capture the majority of surface melt (Fig. 7C). This is because shallow slopes typically have smaller and fewer crevasses than most valley glaciers. They will tend to have the 'flashiest' hydrograph because the supraglacial drainage network rapidly transfers melt off the glacier surface. Interception of this drainage by crevasses or moulins will increase the lag and decrease the amplitude of the hydrograph response.

Our dataset provides new insight into supraglacial channel distribution across a large range of glaciers, allowing simple inferences to be made about connectivity and possible lag times between melt and peak proglacial discharge based on the locations of our mapped channel termini. Overall, we find that at the average Valais glacier, 80% of channels run directly off the glacier, while the remaining 20% terminate in moulins or crevasses. However, this varies between glaciers and in the case of the largest glacier, Grosser Aletschgletscher (type B in Fig. 7), no mapped channels reach the terminus because of highly crevassed zones forcing meltwater into the glacier (53 % of channels enter moulins and 36 % enter crevasses). Unlike most glaciers in the Alps, small supraglacial lakes are also present on the Grosser Aletschgletscher, which capture 11 % of its channels. By comparison, the Oberer Theodulgletscher (type C in Fig. 7), which exhibits the highest drainage density, contains almost no moulins (2.8 % of channel termination), and 27 % of channels reach the terminus or periphery. A large number of channels terminate in crevasses on the Oberer Theodulgletscher (70 %), but crevasses tend to be small (< 0.3 m wide), and it is not known whether meltwater enters englacially or is routed on the glacier surface through trace crevasses (e.g., Fig. 8). Observations have shown that trace crevasses may act as a preferential meltwater pathway, often resulting in channels forming perpendicular to ice flow (e.g., Chen et al., 2024). However, crevasses may also fill with meltwater and be continually overtopped if a channel is situated in a compressive regime, and thus less prone to hydrofracture (e.g., Chudley et al., 2021). As the true location of channel termination is unknown, our channel segments are always broken at crevasses if a clear pathway cannot be identified.

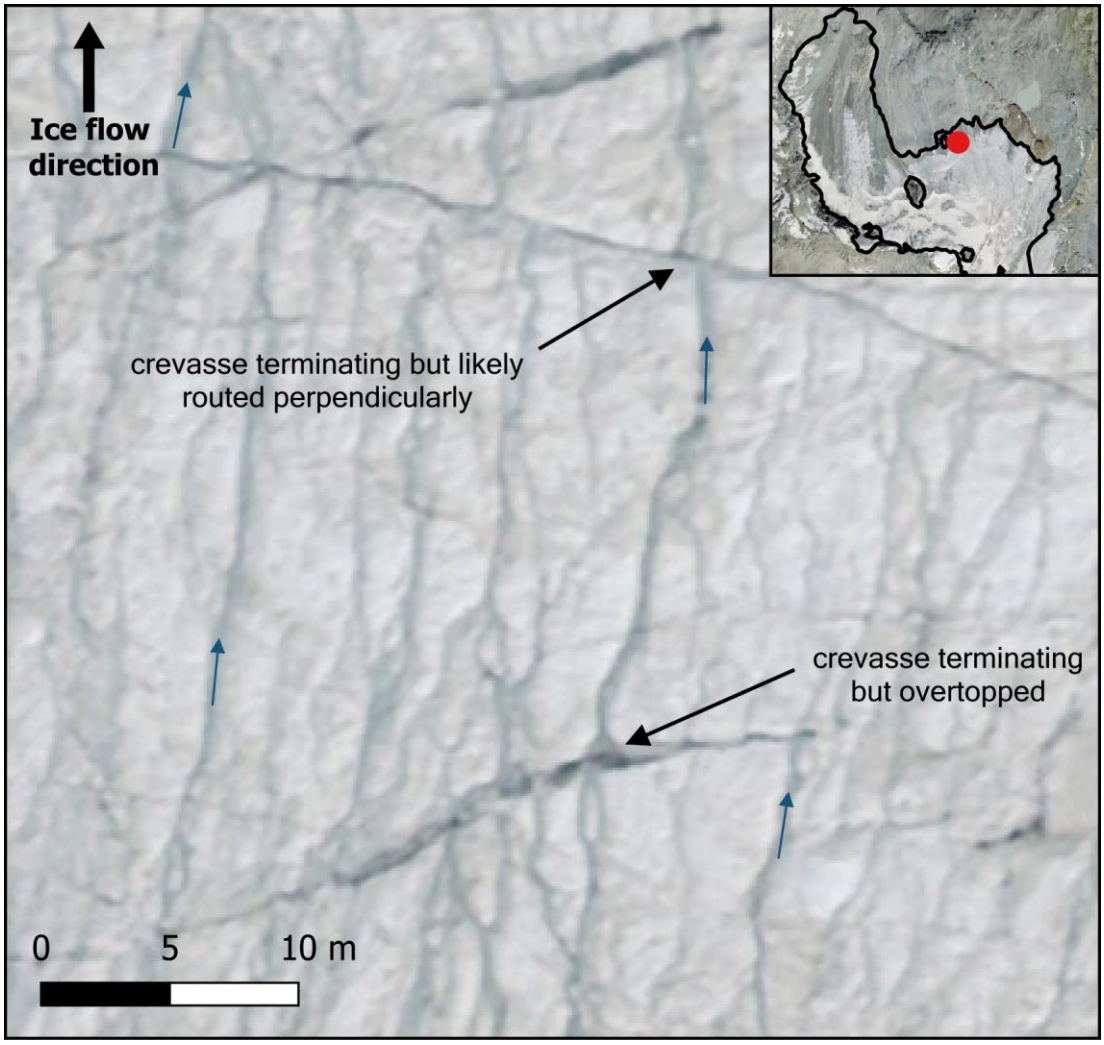

Figure 8: Examples of channels terminating in crevasses on the Oberer Theodulgletscher. The location of the main panel is shown in red on the glacier (top right). Channels are shown to terminate in crevasses but often continue directly down-glacier as some meltwater overtops the crevasse. Small blue arrows indicate the direction of meltwater flow, with meltwater broadly flowing from the bottom to the top of the image. Imagery source: Federal Office of Topography Swisstopo.

The difference in drainage pathways between the Oberer Theodulgletscher and the Grosser Aletschgletscher can be explained by the difference in glacier type outlined in Figure 7. At the Grosser Aletschgletscher, increased meltwater capture by crevasses and moulins likely facilitates increased surface-to-bed meltwater transfer, which is supported by observations of its summer speed-up in ice flow velocity (Leinss and Bernhard, 2021). Model simulations suggest that increased meltwater presence at the glacier bed increases the excavation of subglacial sediment (Delaney and Adhikari, 2020), which would result in higher proglacial stream sediment concentrations if streams are not diluted by freshwater flux from proglacially terminating supraglacial channels. This is important for regions such as the Alps because proglacial stream sediment concentrations can directly impact agriculture and hydropower infrastructure (Micheletti and Lane, 2016). Hence, categorising glaciers based on their slope and

hypsometry is beneficial because it provides insight into the anticipated drainage density of a glacier, probable channel pathways (i.e., sub-/englacially or proglacially terminating), and whether a higher amount of surface-to-bed meltwater transfer is likely.

5.2 Controls on channel morphometry

In Valais, there is a large variation in sinuosity values, with sinuous channels (1.05 - 1.25) occurring on some glaciers but not others. We find that slope affects sinuosity, with the most sinuous channels (2.5 - 1.5) likely to occur on lower angle slopes (0 to 10°) (Fig. 5a); in contrast, channels on steeper slopes (> 20°) typically do not exhibit a sinuosity over 1.3. Channels tend to be least sinuous on debris-free ice, slightly more sinuous on thicker debris cover, and the most sinuous on moderately debris-covered ice (Fig. 5c). However, the most sinuous channels are found on predominantly debris-free ice on Gornergletscher (Fig. 4e). The high prevalence of sinuous channels on moderately debris-covered ice may be due to increased sediment in the channels, sourced from the surrounding terrain, which was also found to increase channel sinuosity at an Alaskan glacier (Boyd et al., 2004). However, the relationship we observe between slope and sinuosity in Valais (Fig. 5a) differs from the findings of St Germain and Moorman (2019), who found that channels on a High Arctic glacier were more sinuous on steeper slopes. This difference may be explained by three factors. The first is that channel distribution in Valais is heavily influenced by crevassed areas (Fig. 5b; Fig. 6), meaning that channel formation is more likely on flatter areas with fewer crevasses. A second consideration is channel discharge, which we do not measure here. Discharge and slope control stream power, which has been found to positively correlate with sinuosity (Ferguson et al., 1973; Marston, 1983; St Germain and Moorman, 2019). We cannot separate out the relative impacts of slope and discharge. However, higher discharges are most likely to form on flatter areas with fewer crevasses, as they favour the development of longer channels (e.g., Fig. 5b). Additionally, reduced meltwater interception in flatter areas allows more meltwater to enter channels, potentially increasing sinuosity. Finally, the sediment cover of many glaciers in Valais exceeds that of the glacier examined by St Germain and Moorman (2019). Hence, channel sediment content is likely higher in Valais, which may increase channel sinuosity due to enhanced erosion during sediment transport or, alternatively, reduce erosion where the bed is covered by thick sediment. Overall, the difference in relationship between slope and sinuosity between Valais and a glacier High Arctic is attributed to the effect of multiple independent variables on sinuosity, which differ in impact between locations.

5.3 Comparison between Valais glaciers and the Greenland Ice Sheet

Previous research on supraglacial channel morphometry has predominantly focused on the GrIS (e.g., Smith et al., 2015; Karlstrom and Yang, 2016; Yang and Smith, 2016; Yang et al., 2016, 2021, 2022), with some similarities in drainage patterns observed between the GrIS and Valais glaciers. For example, in Valais, larger glaciers often contain dendritic drainage patterns (e.g., 4a), which are commonly observed on the GrIS (e.g., Yang et al., 2016, 2019). However, some glaciers in Valais display parallel, weakly interconnected channel networks, likely due to insufficient distance for meltwater to converge into a single channel. It could be expected that, given sufficient distance for meltwater to coalesce, these networks would be comparable to networks on the GrIS, which broadly

follow Horton's laws, i.e., mean river length increases with channel order and mean slope decreases with channel order (Yang et al., 2016). On a smaller scale, ice surface structures (e.g., trace crevasses) exhibit a strong control on meltwater routing on Valais glaciers and on both the Greenland and Antarctic ice sheets (e.g., Fig. 4c; Chen et al., 2024).

Nevertheless, Valais and the GrIS differ in where channels terminate, and their glacier surface characteristics are often dissimilar (e.g., debris coverage). On the southwest GrIS, virtually all higher-order channels terminate in moulins (Smith et al., 2015), whereas at the average Valais glacier, only 20 % of our mapped channels terminate englacially. This suggests notable differences in coupling between surface channels and the englacial/subglacial system. There is also a general absence of supraglacial lakes in Valais, except for small lakes on Gornergletscher and the Grosser Aletschgletscher, meaning few channels terminate in lakes, whereas lakes exist in abundance on the GrIS (Chu, 2014). Additionally, debris cover is more extensive in Valais and is observed to affect channel morphology (see section 5.2) and distribution. The latter is evident from the formation of channels parallel to lateral or medial moraines due to topographic confinement (e.g., Fig. 4b). Debris cover also modulates surface melt and influences both micro-scale and larger-scale surface roughness, which in some cases has been associated with increased channel density (Rippin et al., 2015). However, whilst the scale of sediment coverage differs, the presence of dust, black carbon, algae, and cryoconite deposits on the GrIS may still affect channel distribution and morphometry (e.g., Ryan et al., 2018; Leidman et al., 2021; Khan et al., 2023).

5.4 Future evolution of supraglacial channel systems

The impact of climatic warming on supraglacial drainage networks is not fully understood, but we suggest that supraglacial drainage networks may expand to higher elevations due to rising equilibrium lines (Leeson et al., 2015). Whether discharge in current channels will increase or decrease depends on the rates of glacier retreat and surface lowering, driven by ablation. It is likely that larger glaciers will see an increase in channel discharge due to rising equilibrium lines and associated higher rates of surface melt (St Germain and Moorman, 2019). However, the reduction in area for smaller glaciers may be large enough to prevent the formation of efficient drainage networks. Changes in glacier slope could also result in a reconfiguration of the drainage system (e.g., new crevasses may intercept channels that formerly reached the terminus), which may affect drainage density (Fig. 5e). Additionally, glaciers in some mountain environments are undergoing an increase in debris cover (e.g., Glasser et al., 2016; Fleischer et al., 2021), and it is not fully understood how changes in debris cover will affect surface meltwater supply and transport, channel morphometry and morphology, and surface albedo (e.g., Leidman et al., 2021). Future research could benefit from utilising the growing repository of high-resolution orthophoto surveys to improve our understanding of supraglacial hydrology in mountain glacier settings. Increased understanding of seasonal and interannual channel evolution is needed to better inform modelling of glacier hydrology. For example, it is not clear whether our findings would also apply to regions with larger glaciers and lower rates of surface lowering (e.g., the Arctic), so future studies could repeat our work in such regions. Lastly, further in-situ measurements would be beneficial to determine whether the channels delineated as part of this study represent the majority of meltwater transport on Valais glaciers or whether channels below our mapping resolution also play a key role in meltwater transport.

6 Conclusion

This study presents the first comprehensive dataset on the distribution and characteristics of supraglacial channels at a regional scale in a mountain glacier environment. Out of 285 glaciers in Valais Canton, Switzerland, we identified 85 glaciers that contained channels above our mapping resolution (0.5 m wide). We found substantial variability in glacier drainage density, with the highest values occurring on glaciers with shallow slopes and a large portion of their surface area at lower elevations (Fig. 7). The presence of channels is primarily dictated by a sufficiently supply of meltwater (i.e., large enough glacier area) and an uninterrupted distance for meltwater to coalesce (i.e., absence of crevasses). The primary control on channel distribution is surface topography, with the slope and size of the snow-free area providing a clear limit on both where channels can form and their total length (Fig. 5b). However, strong structural controls on channel distribution exist. For example, trace crevasses have been observed to act as preferential meltwater pathways, resulting in channels forming perpendicular to ice flow. Channels also commonly form parallel to medial and lateral moraines due to topographic confinement. Most channels are characterised by low sinuosity (Fig. 5a), although some highly sinuous channels are present, particularly on moderately debris-covered ice and lower-relief glacier termini. This contrasts with cold or polythermal glaciers, where sinuous channels are more commonly found on steeper slopes. These findings suggest that controls on channel morphology and morphometry are not consistent across mountain glacier environments and may instead reflect variations in debris cover, the location and density of crevassed zones, and rates of surface lowering.

In Valais, most glaciers are characterised by a high proportion of channels that reach the glacier margin without being routed into the glacier. On average, approximately 80 % of channels per glacier run directly off the glacier (terminate proglacially), while the remaining 20 % terminate in a crevasse or moulin. We find that 48 % of glaciers support only proglacially terminating channels, whereas 3.5 % of glaciers are characterised by entirely englacially-terminating channels. The location of channel termini (i.e., proglacial or englacial) is hypothesized to produce different hydrograph responses to surface melt, some of which we suggest may be more common for certain glacier hypsometries (Fig. 7). Channel terminus locations in Valais differ from those described in prior research, which has largely focused on the SW GrIS, where most channels terminate in moulins and very few reach the ice margin. Similar to the GrIS, drainage networks on Valais glaciers often exhibit dendritic patterns. However, such configurations are likely less widespread due to smaller drainage areas and limited distance for channels to merge.

Appendix A: Principal Component Analysis

Table A1: The eigenvectors for principal components 1 to 6 from a PCA analysis of glacier and channel characteristics, with PC1 being the most significant. The three largest loadings for each principal component are in bold.

	PC1	PC2	PC3	PC4	PC5	PC6
Glacier area	**-0.439**	0.042	0.034	0.288	-0.187	0.054
Glacier minimum elevation	**0.435**	-0.112	0.085	-0.098	**0.407**	-0.178
Channel maximum elevation	**0.393**	0.159	0.066	**0.436**	-0.115	0.186
Channel length	-0.070	-0.264	**-0.582**	0.312	0.195	**-0.199**
Channel minimum elevation	0.382	0.196	0.121	**0.423**	-0.100	0.196
Channel sinuosity	-0.117	-0.182	-0.122	-0.041	**0.468**	**0.845**
Channel elevation range	0.166	-0.345	**-0.542**	0.198	-0.173	-0.068
Channel slope	0.320	-0.203	-0.066	-0.115	**-0.483**	**0.255**
Drainage density	0.131	**0.543**	-0.268	-0.009	0.041	0.083
Mean glacier slope	0.119	**-0.439**	0.136	-0.309	-0.335	0.141
Glacier mean elevation	0.170	**-0.376**	**0.401**	0.280	0.339	-0.188
Glacier max elevation	-0.330	-0.175	0.264	**0.462**	-0.163	0.086

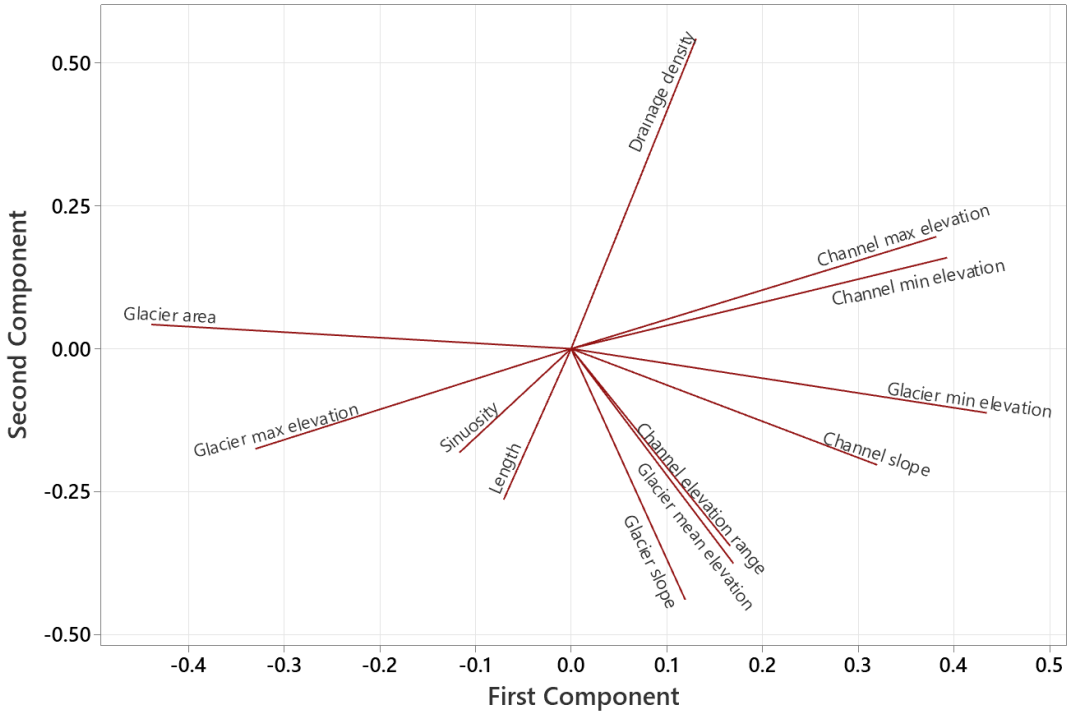

Figure A1: Loading plot for principal components 1 and 2 from a PCA analysis of glacier and channel characteristics.

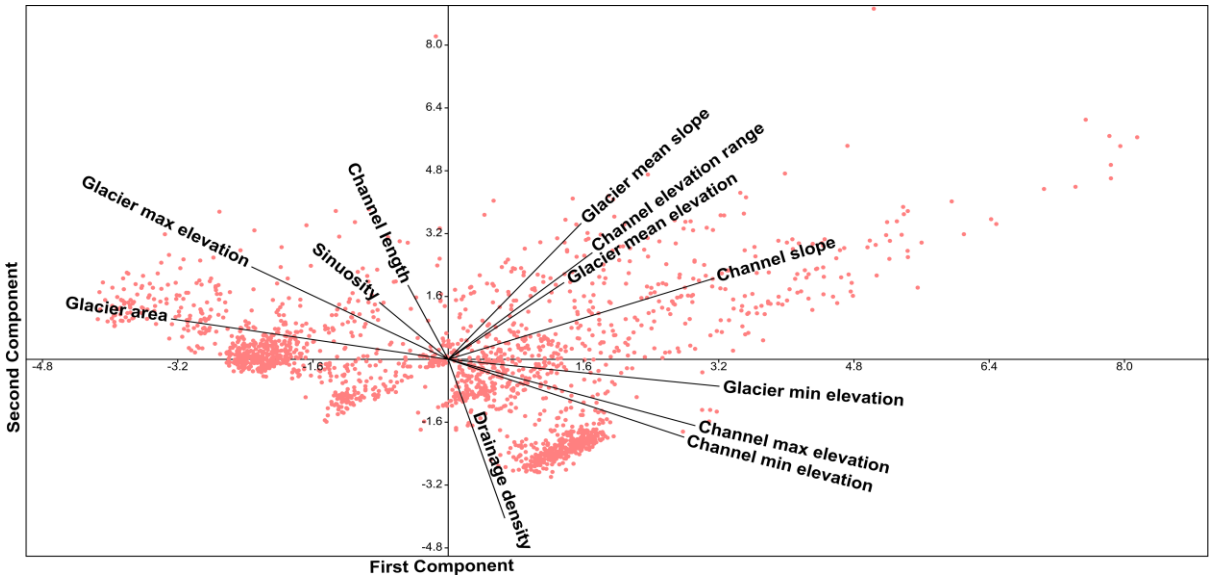

Figure A2: A biplot from a PCA analysis showing principal components 1 and 2, which were used for visually identifying clusters and overlayed with a loading plot (see Fig. A1).

Appendix B: Accuracy Assessment

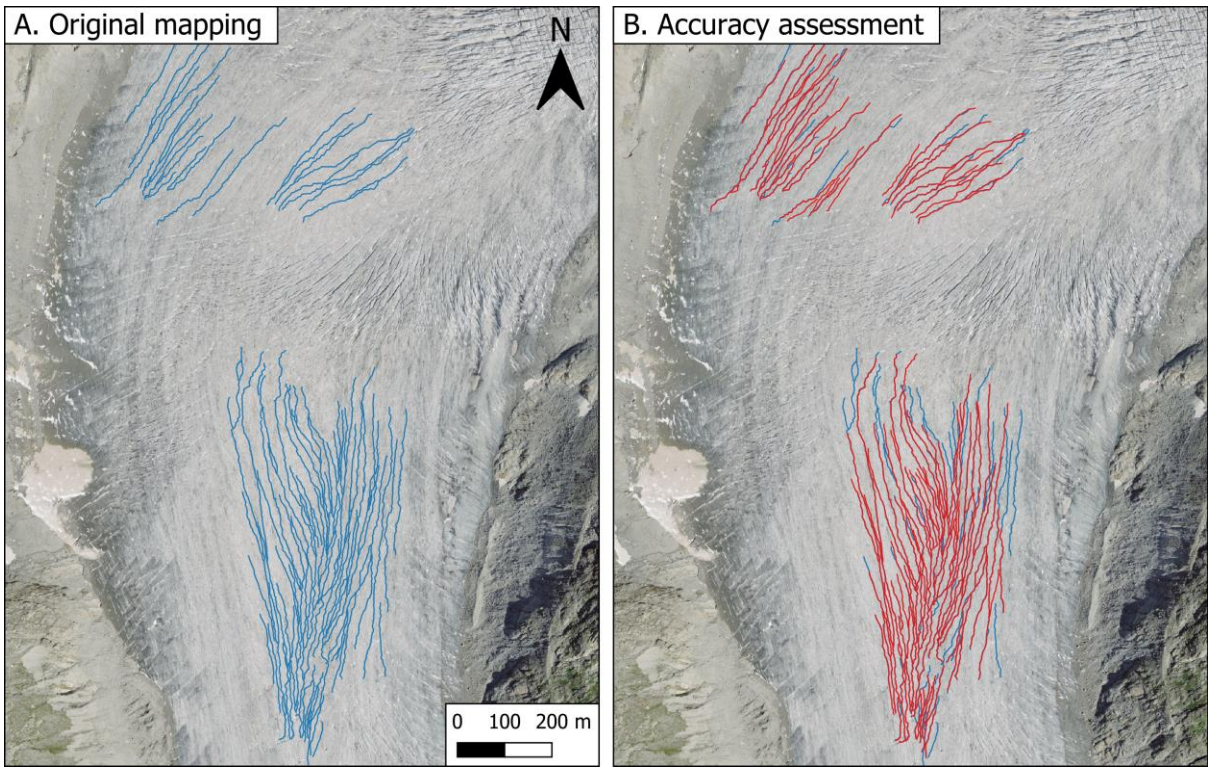

Figure B1: Repeat mapping of the Rhonegletscher used to determine mapping accuracy. (A) Mapping from this dataset is shown in blue. (B) A comparison between the repeat mapping (red) and the original mapping (blue) was undertaken independently after several weeks had elapsed.

Data availability

The orthophoto and DEM data used in this study are freely available on the SwissTopo website (https://www.swisstopo.admin.ch/). Outlines of glaciers in Valais were obtained from Glacier Monitoring in Switzerland (GLAMOS) and are available online (https://glamos.ch/). The produced supraglacial channel data is available upon request from the corresponding author (Holly Wytiahlowsky: holly.e.wytiahlowsky@durham.ac.uk).

Author contributions

All authors contributed to the conceptualisation of this project. HW conducted the mapping, analysis and data visualisation under the supervision of CRS, RAH, CCC and SSRJ. HW led manuscript writing with comments and edits provided by all authors.

Competing interests

CC is a member of the editorial board of The Cryosphere, and CRS was a member at the time of submission.

Acknowledgements

This work was supported by the Natural Environment Research Council via an IAPETUS2 PhD studentship held by Holly Wytiahlowsky (grant reference NE/S007431/1). We thank SwissTopo for making their orthophotos and DEM data open access. We thank two anonymous reviewers and Ian Willis for their constructive feedback, which has helped to improve this paper, and Kang Yang for acting as editor for the manuscript.

7 References

Bamber, J. L., Oppenheimer, M., Kopp, R. E., Aspinall, W. P., and Cooke, R. M.: Ice sheet contributions to future sea-level rise from structured expert judgment, Proc. Natl. Acad. Sci., 116, 11195–11200, doi:10.1073/pnas.1817205116, 2019.

Banwell, A., Hewitt, I., Willis, I., and Arnold, N.: Moulin density controls drainage development beneath the Greenland ice sheet, J. Geophys. Res. Earth Surf., 121, 2248–2269, doi:10.1002/2015JF003801, 2016.

Bell, R. E., Chu, W., Kingslake, J., Das, I., Tedesco, M., Tinto, K. J., Zappa, C. J., Frezzotti, M., Boghosian, A., and Lee, W. S.: Antarctic ice shelf potentially stabilized by export of meltwater in surface river, Nature, 544, 344–348, doi:10.1038/nature22048, 2017.

Brice, J. and Blodget, J.: Countermeasures for Hydraulic Problems at Bridges, Volume 1 – Analysis and Assessment.

Boyd, B., Goetz, S. L., and Ham, N. R.: Supraglacial stream incision into debris-covered ice, Matanuska Glacier, AK. Geol. Soc. Am. Abstr., 36, 11.

Carey, M., Molden, O. C., Rasmussen, M. B., Jackson, M., Nolin, A. W., and Mark, B. G.: Impacts of glacier recession and declining meltwater on mountain societies, Ann. Am. Assoc. Geogr., 107, 350–359, doi:10.1080/24694452.2016.1243039, 2017.

Chen, J., Hodge, R. A., Jamieson, S. S. R., and Stokes, C. R.: Distribution and morphometry of supraglacial channel networks on Antarctic ice shelves. J. Glaciol., doi:10.1017/jog.2024.99, 2024.

Chu, V. W.: Greenland Ice Sheet hydrology: A review, Prog. Phys. Geogr., 38, 19–54, doi:10.1177/0309133313507075, 2014.

Chudley, T. R., Christoffersen, P., Doyle, S. H., Bougamont, M., Schoonman, C. M., Hubbard, B., and James, M. R.: Supraglacial lake drainage at a fast-flowing Greenlandic outlet glacier, Proc. Natl. Acad. Sci., 116, 25468–25477, doi:10.1073/pnas.1913685116, 2019.

Chudley, T. R., Christoffersen, P., Doyle, S. H., Dowling, T. P. F., Law, R., Schoonman, C. M., Bougamont, M., and Hubbard, B.: Controls on Water Storage and Drainage in Crevasses on the Greenland Ice Sheet, J. Geophys. Res. Earth Surf., 126, e2021JF006287, doi:10.1029/2021JF006287, 2021.

Clason, C. C, Coch, C., Jarsjö, J., Brugger, K., Jansson, P., and Rosqvist, G.: Dye tracing to determine flow properties of hydrocarbon-polluted Rabots glaciär, Kebnekaise, Sweden, Hydrol. Earth Syst. Sci., 19, 2701–2715, doi:10.5194/hess-19-2701-2015, 2015.

Clason, C. C, Rangecroft, S., Owens, P. N., Łokas, E., Baccolo, G., Selmes, N., Beard, D., Kitch, J., Dextre, R. M., Morera, S., and Blake, W.: Contribution of glaciers to water, energy and food security in mountain regions: current perspectives and future priorities, Ann. Glaciol., 63, 73–78, doi:10.1017/aog.2023.14, 2023.

Davaze, L., Rabatel, A., Dufour, A., Hugonnet, R., and Arnaud, Y.: Region-wide annual glacier surface mass balance for the European Alps from 2000 to 2016, Front. Earth Sci., 8, doi:10.3389/feart.2020.00149, 2020.

Delaney, I. and Adhikari, S.: Increased subglacial sediment discharge in a warming climate: consideration of ice dynamics, glacial erosion, and fluvial sediment transport, Geophys. Res. Lett., 47, e2019GL085672, doi:10.1029/2019GL085672, 2020.

Dozier, J.: An examination of the variance minimization tendencies of a supraglacial stream, J. Hydrol., 31, 359–380, doi:10.1016/0022-1694(76)90134-7, 1976.

Edwards, T. L., Nowicki, S., Marzeion, B., Hock, R., Goelzer, H., Seroussi, H., Jourdain, N. C., Slater, D. A., Turner, F. E., Smith, C. J., McKenna, C. M., Simon, E., Abe-Ouchi, A., Gregory, J. M., Larour, E., Lipscomb, W. H., Payne, A. J., Shepherd, A., Agosta, C., Alexander, P., Albrecht, T., Anderson, B., Asay-Davis, X., Aschwanden, A., Barthel, A., Bliss, A., Calov, R., Chambers, C., Champollion, N., Choi, Y., Cullather, R., Cuzzone, J., Dumas, C., Felikson, D., Fettweis, X., Fujita, K., Galton-Fenzi, B. K., Gladstone, R., Golledge, N. R., Greve, R., Hattermann, T., Hoffman, M. J., Humbert, A., Huss, M., Huybrechts, P., Immerzeel, W., Kleiner, T., Kraaijenbrink, P., Le clec'h, S., Lee, V., Leguy, G. R., Little, C. M., Lowry, D. P., Malles, J.-H., Martin, D. F., Maussion, F., Morlighem, M., O'Neill, J. F., Nias, I., Pattyn, F., Pelle, T., Price, S. F., Quiquet, A., Radić, V., Reese, R., Rounce, D. R., Rückamp, M., Sakai, A., Shafer, C., Schlegel, N.-J., Shannon, S., Smith, R. S., Straneo, F., Sun, S., Tarasov, L., Trusel, L. D., Van Breedam, J., van de Wal, R., van den Broeke, M., Winkelmann, R., Zekollari, H., Zhao, C., Zhang, T., and Zwinger, T.: Projected land ice contributions to twenty-first-century sea level rise, Nature, 593, 74–82, doi:10.1038/s41586-021-03302-y, 2021.

Esri. "Imagery" [basemap]. Scale Not Given. "World Imagery". October 10, 2024. https://www.arcgis.com/home/item.html?id=10df2279f9684e4a9f6a7f08febac2a9. (October 22, 2024)

Ferguson, R. I.: Sinuosity of supraglacial streams, Geol. Soc. Am. Bull., 84, 251–256, doi:10.1130/0016-7606(1973)84<251:SOSS>2.0.CO;2, 1973.

Fischer, M., Huss, M., and Hoelzle, M.: Surface elevation and mass changes of all Swiss glaciers 1980–2010, Cryosphere, 9, 525–540, doi:10.5194/tc-9-525-2015, 2015.

Fleischer, F., Otto, J.-C., Junker, R. R., and Hölbling, D.: Evolution of debris cover on glaciers of the Eastern Alps, Austria, between 1996 and 2015, Earth Surf. Process. Landf., 46, 1673–1691, doi:10.1002/esp.5065, 2021.

Glasser, N. F., Holt, T. O., Evans, Z. D., Davies, B. J., Pelto, M., and Harrison, S.: Recent spatial and temporal variations in debris cover on Patagonian glaciers, Geomorphology, 273, 202–216, doi:10.1016/j.geomorph.2016.07.036, 2016.

690 Gleason, C. J., Smith, L. C., Chu, V. W., Legleiter, C. J., Pitcher, L. H., Overstreet, B. T., Rennermalm, A. K.,
691 Forster, R. R., and Yang, K.: Characterizing supraglacial meltwater channel hydraulics on the Greenland Ice
692 Sheet from in situ observations, Earth Surf. Process. Landf., 41, 2111–2122, doi:10.1002/esp.3977, 2016.

693 Gleason, C. J., Yang, K., Feng, D., Smith, L. C., Liu, K., Pitcher, L. H., Chu, V. W., Cooper, M. G., Overstreet,
694 B. T., Rennermalm, A. K., and Ryan, J. C.: Hourly surface meltwater routing for a Greenlandic supraglacial
695 catchment across hillslopes and through a dense topological channel network, Cryosphere, 15, 2315–2331,
696 doi:10.5194/tc-15-2315-2021, 2021.

697 Hambrey, M. J.: Supraglacial drainage and its relationship to structure, with particular reference to Charles
698 Rabots Bre, Okstindan, Norway, Nor. Geogr. Tidsskr., 31, 69–77, doi:10.1080/00291957708545319, 1977.

699 Horton, R. E.: Erosional development of streams and their drainage basins; hydrophysical approach to
700 quantitative morphology, Geol. Soc. Am. Bull., 56, 275–370, doi:10.1130/0016-
701 7606(1945)56[275:EDOSAT]2.0.CO;2, 1945.

702 Hugonnet, R., McNabb, R., Berthier, E., Menounos, B., Nuth, C., Girod, L., Farinotti, D., Huss, M., Dussaillant,
703 I., Brun, F., and Kääb, A.: Accelerated global glacier mass loss in the early twenty-first century, Nature, 592,
704 726–731, doi:10.1038/s41586-021-03436-z, 2021.

705 Huss, M., Bauder, A., Werder, M., Funk, M., and Hock, R.: Glacier-dammed lake outburst events of Gornersee,
706 Switzerland, J. Glaciol., 53, 189–200, doi.org:10.3189/172756507782202784, 2007.

707 Immerzeel, W. W., Lutz, A. F., Andrade, M., Bahl, A., Biemans, H., Bolch, T., Hyde, S., Brumby, S., Davies, B.
708 J., Elmore, A. C., Emmer, A., Feng, M., Fernández, A., Haritashya, U., Kargel, J. S., Koppes, M., Kraaijenbrink,
709 P. D. A., Kulkarni, A. V., Mayewski, P. A., Nepal, S., Pacheco, P., Painter, T. H., Pellicciotti, F., Rajaram, H.,
710 Rupper, S., Sinisalo, A., Shrestha, A. B., Viviroli, D., Wada, Y., Xiao, C., Yao, T., and Baillie, J. E. M.:
711 Importance and vulnerability of the world's water towers, Nature, 577, 364–369, doi:10.1038/s41586-019-1822-
712 y, 2020.

713 Irvine-Fynn, T. D. L., Hodson, A. J., Moorman, B. J., Vatne, G., and Hubbard, A. L.: Polythermal glacier
714 hydrology: a review, Rev. Geophys., 49, doi:10.1029/2010RG000350, 2011.

715 Jobard, S. and Dzikowski, M.: Evolution of glacial flow and drainage during the ablation season, J. Hydrol.,
716 330, 663–671, doi:10.1016/j.jhydrol.2006.04.031, 2006.

717 Karlstrom, L. and Yang, K.: Fluvial supraglacial landscape evolution on the Greenland Ice Sheet, Geophys. Res.
718 Lett., 43, 2683–2692, doi:10.1002/2016GL067697, 2016.

719 Khan, A. L., Xian, P., and Schwarz, J. P.: Black carbon concentrations and modeled smoke deposition fluxes to
720 the bare-ice dark zone of the Greenland Ice Sheet, Cryosphere, 17, 2909–2918, doi:10.5194/tc-17-2909-2023,
721 2023.

722 King, L., Hassan, M. A., Yang, K., and Flowers, G.: Flow routing for delineating supraglacial meltwater channel
723 networks, Remote Sens., 8, 988, doi:10.3390/rs8120988, 2016.

724 Kingslake, J., Ely, J. C., Das, I., and Bell, R. E.: Widespread movement of meltwater onto and across Antarctic
725 ice shelves, Nature, 544, 349–352, doi:10.1038/nature22049, 2017.

726 Knighton, A. D.: Channel form adjustment in supraglacial streams, Austre Okstindbreen, Norway, Arct. Antarct.
727 Alp. Res., 17, 451, doi:10.2307/1550870, 1985.

728 Knighton, A. D.: Channel form and flow characteristics of supraglacial streams, Austre Okstindbreen, Norway,
729 Arct. Alp. Res., 13, 295, doi:10.2307/1551036, 1981.

730 Knighton, A. D.: Meandering habit of supraglacial streams, Geol. Soc. Am. Bull., 83, 201–204,
731 doi:10.1130/0016-7606(1972)83[201:MHOSS]2.0.CO;2, 1972.

Leeson, A. A., Shepherd, A., Briggs, K., Howat, I., Fettweis, X., Morlighem, M., and Rignot, E.: Supraglacial lakes on the Greenland Ice Sheet advance inland under warming climate, Nat. Clim. Change, 5, 51–55, doi:10.1038/nclimate2463, 2015.

Leidman, S. Z., Rennermalm, Å. K., Muthyala, R., Guo, Q., and Overeem, I.: The presence and widespread distribution of dark sediment in Greenland Ice Sheet supraglacial streams implies substantial impact of microbial communities on sediment deposition and albedo, Geophys. Res. Lett., 48, 2020GL088444, doi:10.1029/2020GL088444, 2021.

Leigh, J. R., Stokes, C. R., Carr, R. J., Evans, I. S., Andreassen, L. M., and Evans, D. J. A.: Identifying and mapping very small (<0.5 km^2) mountain glaciers on coarse to high-resolution imagery, J. Glaciol., 65, 873–888, https://doi.org/10.1017/jog.2019.50, 2019.

Leinss, S. and Bernhard, P.: TanDEM-X:Deriving InSAR height changes and velocity dynamics of Great Aletsch Glacier, IEEE J. Sel. Top. Appl. Earth Obs. Remote Sens., 14, 4798–4815, https://doi.org/10.1109/JSTARS.2021.3078084, 2021.

Linsbauer, A., Huss, M., Hodel, E., Bauder, A., Fischer, M., Weidmann, Y., Bärtschi, H., and Schmassmann, E.: The new Swiss glacier inventory SGI2016: from a topographical to a glaciological dataset, Front. Earth Sci., 9, doi:10.3389/feart.2021.704189, 2021.

Mantelli, E., Camporeale, C., and Ridolfi, L.: Supraglacial channel inception: modeling and processes, Water Resour. Res., 51, 7044–7063, doi:10.1002/2015WR017075, 2015.

Marston, R. A.: Supraglacial stream dynamics on the Juneau Icefield, Ann. Am. Assoc. Geogr., 73, 597–608, doi:10.1111/j.1467-8306.1983.tb01861.x, 1983.

MeteoSwiss: https://www.meteoswiss.admin.ch/, last access: 1 February 2024.

Micheletti, N. and Lane, S. N.: Water yield and sediment export in small, partially glaciated Alpine watersheds in a warming climate, Water Resour. Res., 52, 4924–4943, doi: 10.1002/2016WR018774, 2016.

Nienow, P., Sharp, M., and Willis, I.: Seasonal changes in the morphology of the subglacial drainage system, Haut Glacier d'Arolla, Switzerland, Earth Surf. Process. Landf., 23, 825–843, https://doi.org/10.1002/(SICI)1096-9837(199809)23:9<825::AID-ESP893>3.0.CO;2-2, 1998.

Pitcher, L. H. and Smith, L. C.: Supraglacial Streams and Rivers, Annu. Rev. Earth Planet. Sci., 47, 421–452, doi:10.1146/annurev-earth-053018-060212, 2019.

Rippin, D. M., Pomfret, A., and King, N.: High resolution mapping of supra-glacial drainage pathways reveals link between micro-channel drainage density, surface roughness and surface reflectance, Earth Surf. Process. Landf., 40, 1279–1290, doi:10.1002/esp.3719, 2015.

Rounce, D. R., Hock, R., Maussion, F., Hugonnet, R., Kochtitzky, W., Huss, M., Berthier, E., Brinkerhoff, D., Compagno, L., Copland, L., Farinotti, D., Menounos, B., and McNabb, R. W.: Global glacier change in the 21st century: Every increase in temperature matters, Science, 379, 78–83, doi:10.1126/science.abo1324, 2023.

Ryan, J. C., Hubbard, A., Stibal, M., Irvine-Fynn, T. D., Cook, J., Smith, L. C., Cameron, K., and Box, J.: Dark zone of the Greenland Ice Sheet controlled by distributed biologically-active impurities, Nat. Commun., 9, 1065, doi:10.1038/s41467-018-03353-2, 2018.

Seaberg, S. Z., Seaberg, J. Z., Hooke, R. L., and Wiberg, D. W.: Character of the englacial and subglacial drainage system in the lower part of the ablation area of Storglaciären, Sweden, as Revealed by Dye-Trace Studies, J. Glaciol., 34, 217–227, doi:10.3189/S0022143000032263, 1988.

Smith, L. C., Chu, V. W., Yang, K., Gleason, C. J., Pitcher, L. H., Rennermalm, A. K., Legleiter, C. J., Behar, A. E., Overstreet, B. T., Moustafa, S. E., Tedesco, M., Forster, R. R., LeWinter, A. L., Finnegan, D. C., Sheng, Y., and Balog, J.: Efficient meltwater drainage through supraglacial streams and rivers on the southwest Greenland Ice Sheet, Proc. Natl. Acad. Sci., 112, 1001–1006, doi:10.1073/pnas.1413024112, 2015.

776 Sommer, C., Malz, P., Seehaus, T. C., Lippl, S., Zemp, M., and Braun, M. H.: Rapid glacier retreat and
777 downwasting throughout the European Alps in the early 21st century, Nat. Commun., 11, 3209,
778 doi:10.1038/s41467-020-16818-0, 2020.

779 St Germain, S. L. and Moorman, B. J.: Long-term observations of supraglacial streams on an Arctic glacier, J.
780 Glaciol., 65, 900–911, doi:10.1017/jog.2019.60, 2019.

781 Swift, D. A., Nienow, P. W., Spedding, N., and Hoey, T. B.: Geomorphic implications of subglacial drainage
782 configuration: rates of basal sediment evacuation controlled by seasonal drainage system evolution, Sediment.
783 Geol., 149, 5–19, doi:10.1016/S0037-0738(01)00241-X, 2002.

784 Tepes, P., Gourmelen, N., Nienow, P., Tsamados, M., Shepherd, A., and Weissgerber, F.: Changes in elevation
785 and mass of Arctic glaciers and ice caps, 2010–2017, Remote Sens. Environ., 261, 112481,
786 doi:10.1016/j.rse.2021.112481, 2021.

787 The GlaMBIE Team: Community estimate of global glacier mass changes from 2000 to 2023, Nature, 1–7,
788 doi:10.1038/s41586-024-08545-z, 2025.

789 Willis, I.C.: Intra-annual variations in glacier motion: a review, Prog. Phys. Geogr., 19.
790 doi:10.1177/030913339501900104, 1995.

791 Wouters, B., Gardner, A. S., and Moholdt, G.: Global glacier mass loss during the GRACE satellite mission
792 (2002-2016), Front. Earth Sci., 7, 2019.

793 Yang, K. and Smith, L. C.: Internally drained catchments dominate supraglacial hydrology of the southwest
794 Greenland Ice Sheet, J. Geophys. Res.-Earth Surf., 121, doi:10.1002/2016JF003927, 2016.

795 Yang, K. and Smith, L. C.: Supraglacial streams on the Greenland Ice Sheet delineated from combined spectral-
796 shape information in high-resolution satellite imagery, IEEE Geosci. Remote Sens. Lett., 10, 801–805,
797 doi:10.1109/LGRS.2012.2224316, 2013.

798 Yang, K., Smith, L. C., Andrews, L. C., Fettweis, X., and Li, M.: Supraglacial drainage efficiency of the
799 Greenland Ice Sheet estimated from remote sensing and climate models, J. Geophys. Res.-Earth Surf., 127,
800 e2021JF006269, doi:10.1029/2021JF006269, 2022.

801 Yang, K., Smith, L. C., Chu, V. W., Gleason, C. J., and Li, M.: A caution on the use of surface digital elevation
802 models to simulate supraglacial hydrology of the Greenland Ice Sheet, IEEE J. Sel. Top. Appl. Earth Observ.
803 Remote Sens., 8, 5212–5224, doi:10.1109/JSTARS.2015.2483483, 2015.

804 Yang, K., Smith, L. C., Chu, V. W., Pitcher, L. H., Gleason, C. J., Rennermalm, A. K., and Li, M.: Fluvial
805 morphometry of supraglacial river networks on the southwest Greenland Ice Sheet, GISci. Remote Sens., 53,
806 459–482, doi:10.1080/15481603.2016.1162345, 2016.

807 Yang, K., Smith, L. C., Cooper, M. G., Pitcher, L. H., As, D. van, Lu, Y., Lu, X., and Li, M.: Seasonal evolution
808 of supraglacial lakes and rivers on the southwest Greenland Ice Sheet, J. Glaciol., 67, 592–602,
809 doi:10.1017/jog.2021.10, 2021.

810 Yang, K., Smith, L. C., Karlstrom, L., Cooper, M. G., Tedesco, M., van As, D., Cheng, X., Chen, Z., and Li, M.:
811 A new surface meltwater routing model for use on the Greenland Ice Sheet surface, Cryosphere, 12, 3791–3811,
812 doi:10.5194/tc-12-3791-2018, 2018.

813 Yang, K., Smith, L. C., Sole, A., Livingstone, S. J., Cheng, X., Chen, Z., and Li, M.: Supraglacial rivers on the
814 northwest Greenland Ice Sheet, Devon Ice Cap, and Barnes Ice Cap mapped using Sentinel-2 imagery, Int. J.
815 Appl. Earth Obs. Geoinf., 78, 1–13, doi:10.1016/j.jag.2019.01.008, 2019.

816 Yang, K., Sommers, A., Andrews, L. C., Smith, L. C., Lu, X., Fettweis, X., and Li, M.: Intercomparison of
817 surface meltwater routing models for the Greenland Ice Sheet and influence on subglacial effective pressures,
818 Cryosphere, 14, 3349–3365, doi:10.5194/tc-14-3349-2020, 2020.

819 Zekollari, H., Huss, M., and Farinotti, D.: Modelling the future evolution of glaciers in the European Alps under
820 the EURO-CORDEX RCM ensemble, Cryosphere, 13, 1125–1146, doi:10.5194/tc-13-1125-2019, 2019.

821 Zemp, M., Huss, M., Thibert, E., Eckert, N., McNabb, R., Huber, J., Barandun, M., Machguth, H., Nussbaumer,
822 S. U., Gärtner-Roer, I., Thomson, L., Paul, F., Maussion, F., Kutuzov, S., and Cogley, J. G.: Global glacier mass
823 changes and their contributions to sea-level rise from 1961 to 2016, Nature, 568, 382–386, doi:10.1038/s41586-
824 019-1071-0, 2019.